

Analysing and assessing the antimicrobial and antioxidant qualities of essential oils and seed extracts of *Anethum graveolens* from southern Morocco using phytochemistry: an in vitro and in silico method for a natural substitute for synthetic preservatives

1. J. SURYA PRAKASH*, Asst. Professor, DEPT OF Pharmacy Practice

2. G. Udaya, Asst. Professor, DEPT OF Pharmacology

3. N. Praveen Kumar, Asst. Professor, DEPT OF PHARMACEUTICS

4. Mr. C. Venku reddy, professor, DEPT OF Pharmacology, SWATHI COLLEGE OF PHARMACY, NELLORE.

5. Dr. M. SREENIVASULU, PRINCIPAL, NARAYANA PHARMACY COLLEGE

^{1,2,3,5} NARAYANA PHARMACY COLLEGE, CHINTHA REDDY PALEM, NELLORE

Abstract: The fragrant shrub *Anethum graveolens* has long been used as a carminative and antispasmodic. Analysing the chemical makeup of the essential oils and extracts derived from seeds collected in Errachidia, southern Morocco, is the aim of this research. The antibacterial and antioxidant qualities of these oils and extracts will also be assessed. The primary constituents of the hydrodistillation-isolated EO were identified by GC-MS analysis as E-anethole (38.13%), es-tragole (29.52%), fenchone (17.21%), and α -pinene (7.37%). The techniques of decoction and Soxhlet were used to extract the phenolic components. *A. graveolens* seeds were found to contain significant quantities of polyphenols, flavonoids, and condensed tannins, with varying levels depending on the extract examined, according to the phenolic compounds test. The most significant compounds found in this extract were umbelliferone (12.35%), 3-hydroxyflavone (11.23%), rosmanol (8.95%), bi-otin (8.36%), emmotin H (4.91%), and coumarin (4.21%), according to HPLC/UV-ESI-MS analysis done on the decoction. According to three methods (DPPH•, FRAP, and CAT), the antioxidant activity showed that the essential oils (EOs) and extracts had a strong ability to combat harmful free radicals, regulate the production of reactive oxygen species, and lessen oxidative damage. Five strains (*E. cloacae*, *K. pneumoniae*, *E. coli*, *S. aureus*, and *S. epidermidis*) and four candidiasis (*C. albicans*, *C. dubliniensis*, *C. tropicalis*, and *C. parapsilosis*) as well as *Aspergillus niger* were tested for the antibacterial activity of the extracts in a liquid medium. The findings demonstrated how efficient the EOs were against the majority of the tested bacteria when compared to aqueous, ethanolic, and decoction extracts. Furthermore, the ethanolic extract exhibited antifungal activity that set it apart from the other extracts. The three main ingredients of the essential oils under investigation—E-anethole, estragole, and fenchone—interact synergistically to produce their antibacterial effectiveness. Important interactions and stability between the chosen bioactive compounds and several target proteins involved in antibacterial and antioxidant activities are also shown by molecular docking and molecular dynamics simulation findings. Better binding energies with the investigated proteins were shown by compounds such as 3-hydroxyflavone, emmotin H, trans-caftaric acid, methylrosmarinic acid, 1-caffeoyl-beta-D-glucose, and kaempferol, suggesting their potential as antioxidants and antimicrobials. Lastly, our results highlight the importance of *A. graveolens* seeds as a viable source of beneficial health substances that may act as natural alternatives to the currently used artificial preservatives.

Keywords: *Anethum graveolens*; GC/MS; HPLC/UV-ESI-MS; polyphenols; flavonoids; antioxidants; antimicrobials

1. Introduction

Foodborne infections are a major global public health concern that have a huge socioeconomic effect, particularly in underdeveloped nations [1]. According to the World Health Organisation (WHO), antibiotic resistance led to 4.95 million deaths in 2023 and caused 1.27 million deaths worldwide in 2019. A lot of research is being done to create novel antibacterial agents and nutritious food items in response to these concerning tendencies.

However, because of their toxicity and induction of DNA damage, the use of synthetic preservatives like BHA and BHT to prevent food degradation has been banned [2,3]. According to this viewpoint, customers are worried about their detrimental impacts on human health. Because of this, businesses and consumers are now looking for and consuming natural derivatives that have antibacterial and antioxidant qualities. The

essential oils and extracts from therapeutic plants are among these natural compounds. These plants are thought to be a major source of secondary metabolites that are active and have therapeutic qualities. These substances are mostly engaged in defence mechanisms against herbivores, pathogens, and their rivals [4]. Pharmaceuticals, agriculture, cosmetics, and industrial raw materials are just a few of the areas to which plants have made remarkable and varied contributions. In fact, they serve two main purposes: first, they give food a pleasing flavour; second, they preserve food by delaying its degradation via their antibacterial and antioxidant properties. *Anethum graveolens* is a common plant utilised in the pharmaceutical and agri-food industries, referred to as "dill" [5]. This plant is the only member of the *Anethum* genus and a perennial herbaceous species in the Apiaceae family. It usually

grows between 40 and 60 centimetres in height. The important plant dill is grown in the Mediterranean and Asiatic regions. For five thousand years, the Egyptians and Greeks have used its seeds and leaves as a traditional spice to flavour food [6]. Dill is often used in traditional medicine to relieve newborn colic and young children's flatulence. Furthermore, its seed is utilised in decoction or infusion mode to treat gastrointestinal spasms, diarrhoeal diseases with meteorism, sleeplessness, hyposecretion of milk, and urinary infections [6,7]. It is often used in the industry as a natural flavour enhancer in a variety of culinary products, especially in sauces, salads, soups, seafood, meats, fries, and pickles. Because of its pleasant scent, volatile oil extracted from the aboveground section is used as a flavour enhancer in culinary and beverage applications. Additionally, essential oils are used as fragrances to improve the aroma of cosmetics, soaps, and detergents [8,9].

Numerous earlier investigations have shown the biological potential of *Anethum Graveolens* at the scientific level. These include anti-inflammatory [10], antidiabetic [11], antimicrobial [12], diuretic [13], insecticidal [14], hepatoprotective [15], anticancer, and antioxidant [16].

Because of its fascinating traits, this species' economic importance has significantly increased on a worldwide scale. This plant has therapeutic, ecological, and socioeconomic value in Morocco. The chemical makeup and biological features of the essential oils extracted from *Anethum graveolens*, which is native to Morocco, are, however, little understood. In particular, our research looked closely at the chemical components found in the essential oil and extracts of *Anethum Graveolens* seeds from the Boulemane region. Additionally, our research sought to identify naturally occurring chemical compounds with antioxidant properties, evaluate the antioxidant, and employing in vitro research to determine the extracts' and essential oils' antimicrobial properties. The chemical makeup of extracts made from *Anethum graveolens* seeds has, however, seldom been the subject of considerable investigation. In order to contribute to the phytochemical analysis and characterisation of chemical families identified in *Anethum graveolens* seeds harvested from the Boulemane area, this research was carried out within the designated context. To discover the essential oils' and extracts' potential as antioxidants and antimicrobials, it also involves evaluating their antibacterial and antioxidant qualities using in vitro and in silico techniques.

2. Results & Discussion

Quality Control of Plant Material

The quality control findings of the examined plant material are displayed in Table 1. These seeds of *A. graveolens* had a moisture content of around 15.80%, which was within the typical range for seeds. The plant extract had a pH that was somewhat acidic, which aligned with its mineral content of 15.03%. This pH level meets the quality criteria set by AFNOR (NF ISO 5984).

Table 1. Analysis and quality control of *A. graveolens* seeds.

MC (%)	pH	Ash (%)	Organic Mafler (%)
15.03	84.97	15.80	5.2

Despite their health benefits, medicinal plants are often contaminated during cultivation and processing by various agents or toxic substances. Heavy metals are the most concerning of them since they may interfere with the healthy functioning of the liver, lungs, heart, kidneys, brain, and central nervous system. Hypertension, stomachaches, skin rashes, intestinal ulcers, and various cancers may all be brought on by this disturbance. We used atomic absorption spectroscopy to measure the concentrations of six distinct heavy metals—chromium (Cr), lead (Pb), cadmium (Cd), iron (Fe), antimony (Sb), and titanium (Ti)—in order to address this issue. Aneth seeds have a high level of iron (Fe) at 0.5858 mg/L, followed by antimony (Sb) at 0.0087 mg/L, according to the data shown in Table 2. Notably, all of the other heavy metals found are within the permissible limit established by FAO/WHO regulatory criteria. Therefore, the plant under study may be used directly, as a component in food processing, or repackaged if necessary.

Table 2. Heavy metal concentration (mg/L) and maximum limit FAO/WHO (2009).

Element	Heavy Metal Content (mg/L)	Maximum Limit
Chromium (Cr)	0.0008	2
Antimony (Sb)	0.0134	1
Lead (Pb)	0.0034	3
Cadmium (Cd)	<0.0001	0.3
Iron (Fe)	0.5858	20
Titanium (Ti)	0.0082	-

Physical-Chemical Properties and Extraction Yield of Essential Oils

According to the information in Table 3, the essential oils (EOs) extracted from *A. graveolens* seeds collected in the Errachidia area during full bloom were distinguished by their fragrant fragrance, yellowish colour, and $2.73 \pm 0.12\%$ yield. This finding was noteworthy since, on the one hand, it was considerable in comparison to those from other countries, such as Egypt (1.88%) [17], India (1.5%) [9], Iran (0.04–1.86%) [18], and also within 1.92% in the same nation [19]. However, it was lower than those found elsewhere, such as in China (6.7%) [21] and southern Morocco (3.5%) [20]. Several genetic, ecological, and environmental factors (plant age, climatic conditions, soil type, growth stage of the species, part used, harvest time, drying process, harvest period and environment, and cultural practices) as well as the extraction method employed are responsible for the variation in EO yield, according to the results of this study and those found in the literature. Essential oils from the plant under study had a density of 0.9362 ± 0.0732 g/mL. According to the 2005 AFNOR standard, essential oils should have a density between 0.906 g/mL, which denotes lower-grade oils, and 0.990 g/mL, which suggests very high-quality oils. According to the test, our essential oil's density is comfortably within the permitted range, suggesting a quality that either meets or surpasses the typical requirements for essential oil density. This finding implies that the essential oil that is derived from this plant has a commendable quality that satisfies industrial requirements.

Table3.EssentialOilYieldof*A.graveolens*.

Properties	Yield(%)	Color	Odor	Density(g/mL)
Results	2.73± 0.12	Yellowish	Aromatic	0.9362± 0.0032

ChemicalCompositionofEO

Thechemicalprofile(SupplementaryFigureS1)revealedthepresenceof29chemical compoundsforthetotalchemicalcompositionofthisessentialoil.Theseresultsareshummarized in Table 4.

Table4.ChemicalCompositionof*Anethumgraveolens*Essential Oil.

N°	Compounds	KI*	RA%	Formula
1	α -Pinene	939	7.37	C ₁₀ H ₁₆
2	Camphene	954	0.08	C ₁₀ H ₁₆
3	Sabinene	975	0.13	C ₁₀ H ₁₆
4	β -Pinene	979	0.35	C ₁₀ H ₁₆
5	Myrcene	990	0.76	C ₁₀ H ₁₆
6	α -Phellandrene	1002	0.17	C ₁₀ H ₁₆
7	α -Terpinene	1017	0.02	C ₁₀ H ₁₆
8	Limonene	1029	1.24	C ₁₀ H ₁₆
9	β -Phellandrene	1029	0.37	C ₁₀ H ₁₆
10	Z- β -Ocimene	1037	0.16	C ₁₀ H ₁₆
11	1,8-Cineole	1031	0.11	C ₁₀ H ₁₈ O
12	γ -Terpinene	1059	0.66	C ₁₀ H ₁₆
13	Terpinolene	1088	0.05	C ₁₀ H ₁₆
14	Fenchone	1086	17.21	C ₁₀ H ₁₆ O
15	Linalool	1096	2.68	C ₁₀ H ₁₈ O
16	trans-Pinenehydrate	1122	0.03	C ₁₀ H ₁₈ O
17	Camphor	1146	0.35	C ₁₀ H ₁₆ O
18	Terpinen-4-ol	1177	0.13	C ₁₀ H ₁₈ O
19	Estragole	1196	29.32	C ₁₀ H ₁₂ O
20	Carvone	1243	0.01	C ₁₀ H ₁₄ O
21	Z-Anethole	1252	0.06	C ₁₀ H ₁₂ O
22	ρ -Anisaldehyde	1250	0.05	C ₈ H ₈ O ₂
23	E-Anethole	1284	38.13	C ₁₀ H ₁₂ O
24	α -Copaene	1376	0.02	C ₁₅ H ₂₄
25	Z-Isoeugenol	1407	0.02	C ₁₀ H ₁₂ O ₂
26	Methyleugenol	1403	0.34	C ₁₁ H ₁₄ O ₂
27	GermacreneD	1481	0.09	C ₁₅ H ₂₄
28	δ -Cadinene	1523	0.03	C ₁₅ H ₂₄
29	E-Methylisoeugenol	1492	0.06	C ₁₁ H ₁₄ O ₂
			%HydrogenatedMonoterpenes	11.36
			%Oxygenated Monoterpenes	20.57
			% Phenylpropanoids	67.93
			%HydrogenatedSesquiterpenes	0.14
			Total	100

*RA:Relativeabundance(%);KI:Kovats index.

According to the chemical composition analysis, phenylpropanoids made up the majority of the compounds found in the essential oil of *Anethum graveolens*, accounting for 67.93%. Monoterpenes,

which were split between oxygenated monoterpenes (20.57%) and hydrogenated monoterpenes (11.36%), came next. Although they were found in little amounts (0.14%), hydrogenated sesquiterpenes were also

detected.

Additionally, ethers made up a large portion of the *A. graveolens* essential oil's chemical makeup (68.04%), with ketones coming in second at 17.57%. Additionally, we observe the presence of alcohol (2.84%) and hydrocarbons (11.5%). Aldehydes, however, were almost absent (0.05%) (Figure 1).

(E)-anethole (38.13%), estragole (29.32%), fenchone (17.21%), and α -pinene (7.37%) made up the majority of the essential oil that was extracted from the seeds of *A. graveolens*. Other compounds, such as linalool (2.68%) and limonene (1.24%), were found in trace levels (Table 4 and Supplementary Figure S2).

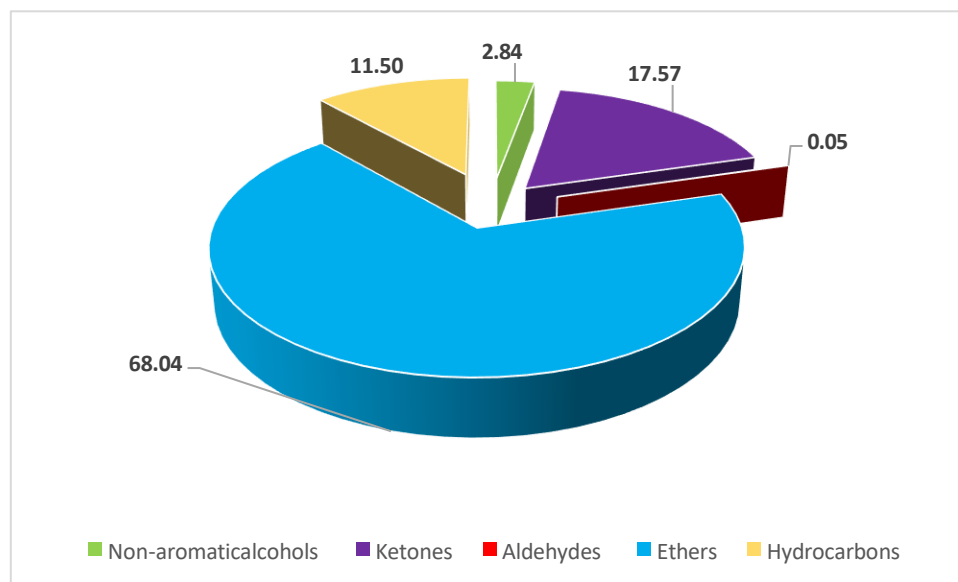


Figure 1. Distribution of the main chemical groups in the essential oil of *A. graveolens*.

The chemical makeup of our *A. graveolens* essential oil varies from that reported in earlier studies of various sources, according to a study of the data, with both qualitative and quantitative changes in individual components detected. In fact, we discovered an intriguing chemical polymorphism in the plant under study.

Few research have examined the chemical makeup of dill essential oil in Morocco. Twelve compounds, accounting for 98% of the essential oil extracted from seeds from southern Morocco, were discovered by Znini et al. [20]. The main constituents were carvone (43.5%), dillapiole (26.7%), and limonene (15.4%). Additionally, chromatographic and El-Sayed et al. [17] used spectrophotometric tests on the essential oil extracted from Egyptian seeds and found that the main constituents of dill essential oil were carvotanacetone (13.03%), D-limonene (19.47%), and dillapiole (44.01%). Carvone (27%), piperitone (25.7%), limonene (20.6%), dillapiole (8%), trans-dihydrocarvone (4.9%), and camphor (4.4%) were reported by Snuossi et al. [22] in Tunisia.

Limonene (48.05%), carvone (37.94%), cis-dihydrocarvone (3.5%), and trans-carvone (1.07%) make up the majority of French essential oil in Europe. [23]. According to Kostić et al. [24], the composition of Dill essential oil from Serbia was completely devoid of phenylpropanoids and dominated by oxygenated monoterpenes (52.79%). The latter had high levels of limonene (29.04%), α -phellandrene (13.12%), and

carvone (42.47%). In the meanwhile, Aati et al. [25] discovered that the essential oil recovered from seeds using the solid-phase microextraction technique Headspace was high in monoterpenes (65.1%) in Asia and Saudi Arabia. Anethole (33.3%), limonene (30.8%), carvone (17.7%), and trans-dihydrocarvone (12.2%) were also among its main constituents. Linalool (63.41%), δ -terpinene (4.27%), β -pinene (3.97%), p-cymene (3.35%), geranyl acetate (3.32%), octyl butyrate (3.3%), and α -pinene (3.23%) are all found in Iranian dill essential oil, according to a research. [26]. However, Najafzadeh et al. [14] discovered that the primary components of this species were para-cymene (5.50%), α -terpineol (5.58%), limonene (21.47%), carvone (23.67%), and phellandrene (34.19%). In China, D-carvone (40.36%), D-limonene (19.31%), apiole (17.50%), α -pinene (6.43%), 9-octa-decanoic acid (9.00%), and 9,12-octadecadienoic acid (2.44%) are the main components of this essential oil under study [21]. Similarly, in India, Kaur et al. [9] reported that the primary compounds in the essential oil of this species were carvone (41.15%), limonene (23.11%), camphor (9.25%), and dihydrocarvone (3.75%), while the minor compounds were butyl acetate (2.65%), myrcene (2.365%), anethole (1.65%), α -pinene (1.06%), and anethole ether (1.02%). The varied plant development phases, the cultivation area, and the particular plant portion employed all influence the distinct components reported by various

research. Screening for phytochemicals using particular revealing reagents, phytochemical assays were performed on a variety of extracts made from *A. graveolens* seeds. Table 5 reports the findings of the phytochemical screening. In varying amounts, this species was abundant in proteins, lipids, reducing sugars (glucose and fructose), polysaccharides, and other primary metabolites. Flavonoids, tannins, mucilages, leuco-anthocyanins, oses and holosides, steroids, and triterpenes were among

the secondary metabolites that were also found to be present. Alkaloids and saponins, however, were not present.

Our findings are in line with those of El Mansouri et al. [27], who found that dill seeds from Southern Morocco lacked saponins and were rich in flavonoids and tannins. The existence of phenolic substances, flavonoids, tannins, and terpenoids was also shown by Kauretal [9].

Table 5. Results of phytochemical tests conducted on extracts of *A. graveolens* seeds.

	Chemical Group	<i>A. graveolens</i>
	Polysaccharide	starch
	Reducing sugars	+
	Biuret reaction	+
Protein	Xanthoprotein reaction	+
Lipids (Lieberman Burchard reaction)	+++	
Tannins	+++	
Catechictannins	++	
	Gallic tannins	++
	Flavonoids	++
	Leucoanthocyanins	++
	Saponosides	-
	Alkaloids	-
	Reducing Compounds	++
	Oses and holosides	++
	Mucilages	++
	Sterols and triterpenes	++

+++ Very abundant; ++: abundant; + weak; - absent.

Phenolic Compound Yields of Extracts

We were able to determine the yield of several phenolic compounds found in the plant under investigation by extracting them. The extracts included ethanol, aqueous, and decocted extracts. The yield was calculated as a percentage relative to 30 g of the plant material that had been dried and powdered. The findings are depicted in Figure 2.

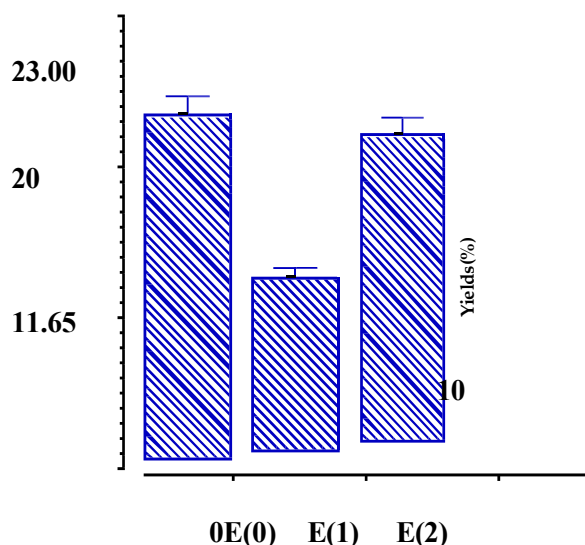


Figure2. Yields of extracts obtained from *A. graveolens*.

The findings demonstrated that extraction yields were influenced by both the extraction technique and the extraction solvent. In fact, the phenolic compounds' average extraction yields varied somewhat and were greater in the aqueous extract ($20.52\% \pm 0.006$) and decocted extract ($23.00\% \pm 0.04$) than in the ethanol extract ($11.65\% \pm 0.003$). When compared to ethanol, we found that water had a tendency to extract more compounds. Water's natural capacity to remove a wide variety of molecules selectively due to its high polarity may be the cause of this phenomena. This comprises a significant amount of non-phenolic compounds, such as proteins and carbohydrates. Content of Flavonoids, Condensed Tannins, and Phenolic Compounds The results obtained from the use of a UV-visible spectrophotometer regarding the amounts of flavonoids and total phenolic components in extracts made from *A. graveolens* seeds are shown in Figure 3. It seemed from the observed data that there was a considerable variance in the quantities of these chemicals among the various extracts. The greatest levels of phenolic components, flavonoids, and tannins were obtained in the ethanolic extract at around 52.65 ± 0.22 mgGAE/gofextract and 35.58 ± 2.79 mgQE/gof. The aqueous extract showed values of 39.72 ± 0.00 mgGAE/gofextract, 13.79 ± 0.63 mgQE/gofextract, and 0.075 ± 0.002 mgCE/gofextract, respectively. The lowest quantities of the studied molecules were obtained by the decoction process, namely 23.35 ± 0.66 mgGAE/gofextract for phenolic compounds, 9.40 ± 0.51 mgQE/gofextract for flavonoids, and 0.046 ± 0.003 mgCE/gofextract for tannins. Compared to El Mansouri et al.'s published findings, ours are much better. [27]. Comparing the decoction to a prior study, we

found that it had somewhat less tannin but larger amounts of flavonoids and phenolic chemicals. According to El Mansouri et al. [27], the concentrations of polyphenol and tannin in the dill seed decoction were 6.16 mg GAE/g of extract and 0.21 mg CE/g of extract, respectively. This disparity highlights the variation in phytochemical content brought about by elements including the extraction process, geographic source, and analytical methodologies.

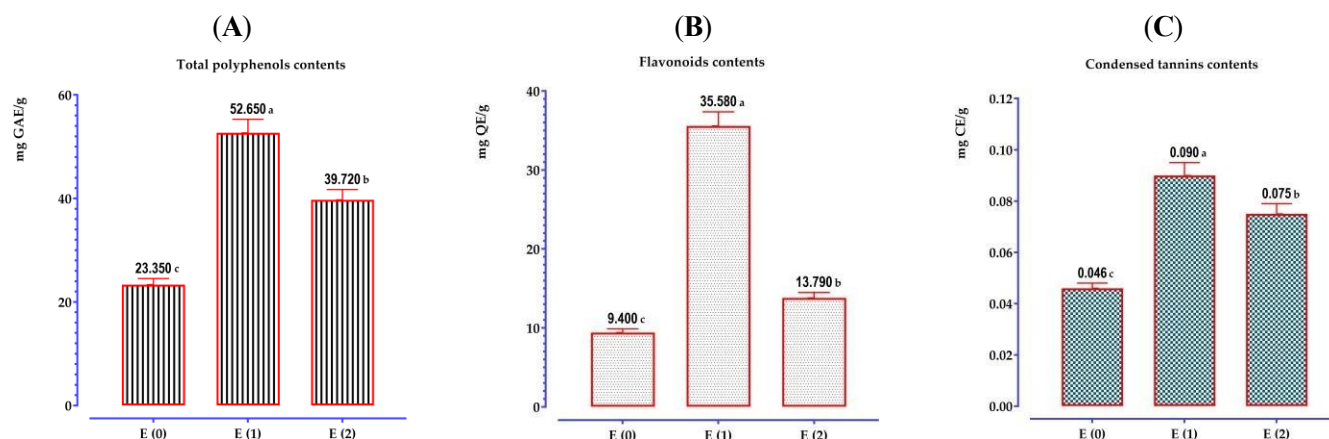


Figure 3. Contents of total polyphenols (A), flavonoids (B), and condensed tannins (C) in extracts from *A. graveolens* seeds. The values are means \pm SD. Results with different superscripts are significantly different from each other ($p < 0.05$).

Chromatographic Analysis by HPLC/UV-ESI-MS of the Extracts

The chromatographic profile, depicted below (Supplementary Figure S3), illustrates the peaks of compounds derived from the decoction of *A. graveolens* seeds, along with their retention times and relative abundances.

Using analytical and spectral data in negative and positive modes, we identified 38 compounds whose names and molecular formulas are presented in Table 6.

Table 6. List of compounds identified by HPLC/UV-ESI-MS in the decoction E(0) of *A. graveolens* seeds.

N°	RT	Area (%)	Molecules	Structure	Classes	Exact Weights	[M-H] ⁻ (m/z)	[M+H] ⁺ (m/z)	Fragment Ions (m/z)
1	4.05	1.8	Medioresinol	C ₂₁ H ₂₃ O ₇	Flavonoid	388	387		207-179
2	4.23	1.75	Caffeic acid	C ₉ H ₈ O ₄	Phenolic acid	180		181	181-163-145-139-114
3	4.33	2.47	Cinnamic acid	C ₉ H ₈ O ₂	Phenolic acid	148	147		119-103-93
4	4.51	1.21	Scopoletin	C ₁₀ H ₈ O ₄	Coumarin	192	191		176-148-104
5	4.75	3.58	Pimelic acid	C ₇ H ₁₂ O ₄	Fatty acid	160	159		115-97
6	5.34	0.53	Retusin	C ₁₉ H ₁₈ O ₇	Flavonoid	358	357		357-342-327-312-297
7	8.39	0.60	Syringic acid	C ₉ H ₁₀ O ₅	Phenolic acid	198	197		179-135-123
8	8.53	1.30	Carnosic acid	C ₂₀ H ₂₇ O ₄	Diterpene	332		333	333-287
9	8.96	12.35	Umbelliferone	C ₉ H ₆ O ₃	Coumarin	162	161		133-106
	109.00	8.36	Biotin	C ₁₀ H ₁₆ N ₂ O ₃					
S									
	Vitamin	244		243	297-228-174-130				
	119.24	4.21	Coumarin	C ₉ H ₆ O ₂	Coumarin	146		147	147-103
	129.48	1.34	Kaempferide	C ₁₆ H ₁₂ O ₆	Flavonoid	300	299		217-149-107
	139.91	11.23	3-Hydroxyflavone	C ₁₅ H ₁₀ O ₃	Flavonoid	238	237		237-135-101
	1410.15	8.95	Rosmanol	C ₂₀ H ₂₆ O ₅	Polyphenol	346	345		243-197-147
	1510.78	3.40	Homovanillic acid	C ₉ H ₁₀ O ₄	Other	182	181		137-123-108
	1611.08	3.35	kaempferol	C ₁₅ H ₁₀ O ₆	Flavonoid	286	285		201-165-151-117
	1711.37	3.56	Methylrosmarinat	C ₁₉ H ₁₈ O ₈	Polyphenol	374		375	375-181-137
	1811.55	0.98	Chlorogenic acid	C ₁₆ H ₁₈ O ₉	Phenolic acid	354	353		191-179
19	12.33	0.55	Apigenin 7-rhamnoside	C ₂₁ H ₂₀ O ₉	Flavonoid	416		417	417-271-243-229
20	12.71	1.02	Quercetin 7-glucuronide	C ₂₁ H ₁₈ O ₁₃	Flavonoid	478	477		431-301-175
	2112.99	0.42	Epicatechingallate	C ₂₂ H ₁₈ O ₁₀	Polyphenol	442	441		289-169-125

2213.72	1.26	Rhamnetin	C ₁₆ H ₁₂ O ₇	Flavonoid	316	315	300-179-165-151	
2313.92	0.42	Riboflavin	C ₁₇ H ₂₀ N ₄ O ₆	Vitamin	376	375	375-255-243-241	
24	14.11	1.29	Quercetin-3-O-galactoside	C ₂₁ H ₂₀ O ₁₂	Flavonoid	464	465	465-427-303-91
25	14.80	1.29	Quercetin3-O-rhamnoside	C ₂₁ H ₂₀ O ₁₁	Flavonoid	448	447	301-300-284
2615.25	1.67	δ-tocopherol	C ₂₇ H ₄₆ O ₂	Vitamin	402	401	385-135	
2715.73	3.85	trans-caftaricacid	C ₁₃ H ₁₂ O ₉	Phenolicacid	312	311	249-203-179-149	
2816.10	1.03	3-Feruloylquinicacid	C ₁₇ H ₂₀ O ₉	Phenolicacid	368	367	293-209-193-173	
2916.60	0.56	Quercetin3,3'-dimethylether	C ₁₇ H ₁₄ O ₇	Flavonoid	330	329	314-301-285-270	
30	17.35	1.62	Rosmarinicacid	C ₁₈ H ₁₆ O ₈	Phenolicacid	360	361	181-163-145-135-117
31	19.06	1.23	Apigenin	C ₁₅ H ₁₀ O ₅	Flavonoid	270	269	227-159-121-105 431-385-268-240-151
32	20.26	0.78	Apigenin-7-glucoside	C ₂₁ H ₂₀ O ₁₀	Flavonoid	432	431	107
33	20.41	0.80	Folicacid	C ₁₉ H ₁₉ N ₇ O ₆	Vitamin	441		311-267-224-175
35	21.43	4.91	EmmotinH	C ₁₅ H ₁₆ O ₃	Sesquiterpenoid	244	243	223-228-200-184
3623.74	0.47	caffeoyl-feruloyltartaric acid	C ₂₃ H ₂₀ O ₁₂	Phenolicacid	488	487	487-443-293	
3725.35	3.37	1-Caffeoyl-beta-D-glucose	C ₁₅ H ₁₈ O ₉	Polyphenol	342	341	341-179-135	
3825.76	0.45	Ascorbylpalmitate	C ₂₂ H ₃₈ O ₇	Other	414	415	415-371-115	

The structural variety of the molecules that make up the dill extract was revealed by the analysis of the data acquired from the decoction. In fact, we found a number of compounds, but the most important ones were two coumarins, umbelliferone (12.35%) and coumarin (4.21%), a sesquiterpenoid called emmotin H (4.91%), a 3-hydroxyflavone flavonoid (11.23%), a diterpene called rosmanol (8.95%), and a vitamin B7 biotin (8.36%). Electrospray ionization-mass spectrometry, or ESI-MS, is an essential method for determining a compound's structure. Each component may be analysed using fragmentation in both positive and negative ion modes. The ESI-MS spectra of umbelliferone revealed that this molecule experienced deprotonation, which led to the loss of a proton (H⁻) and the formation of the [M-H]⁻ ion, which was discovered in the mass spectrometer at 8.96 minutes and observed at m/z=161. Additionally, the main fragments found at m/z = 133 and 106, respectively, characterised the typical fragmentation of the coumarin structure by separating an acetate (CH₃CO) group and a carbon monoxide (CO) group. Similarly, 3-hydroxyflavone (C₁₅H₁₀O₃, M=238), which appears at 9.91 minutes and is accompanied by significant fragments at m/z=237,135, and101 that indicate the fragmentation of the flavonoid structure, including the release of a CO group and a fragment of C₅H₄O₂. Additionally, Rosmanol detected a [M-H]⁻ ion at m/z=345 at 10.15 minutes, with the main pieces at m/z=243 and197, demonstrating the distinctive

fragmentation of its spolyphenolic structure. Additionally, a [M+H]⁺ ion at m/z=243 was used to identify biotin. It occurred at 9.00 min and was followed by fragments at m/z = 297, 228, 174, and 130 that attest to its specific fragmentation. The loss of a portion of the biotin's side structure, maybe including the absence of an available group or a segment of the imidazole, might cause the ion at m/z=297. The loss of a C₃H₈NS group, comprising a piece of the nitrogen and the thiol group, may be the cause of the fragment at m/z = 228. Lastly, the loss of a C₄H₆NO₂ group, which is probably connected to a portion of the imidazole or the valeric acid, might cause the ion at m/z=174. The same was true for emmotin H (C₁₅H₁₆O₃, M = 244), which was detected at 21.43 minutes with a [M-H]⁻ ion at m/z = 243 and fragments at m/z = 243, 228, 200, and 184 that were indicative of the fragmentation unique to its sesquiterpenoid structure. In accordance with negative mass spectrometry procedures, the ion at m/z = 243 revealed a loss of a proton during ionisation and matched the parent [M-H]⁻ ion of the emmotin H molecule. The dissociation of a CH₂(methylene) group, a common finding in sesquiterpenoids, may be the cause of the fragment at m/z=228. A more significant loss in the carbon chain may also be indicated by the fragment at m/z=200, which may be connected to the cleavage of an alkene group or another functional group. Lastly, further fragmentation of these sesquiterpenoids' skeleton, most likely including the loss of a less complicated structure,

may be the cause of the ion at $m/z = 184$. Finally, after 9.24 minutes, coumarin (C₉H₆O₂, M = 146) displayed a [M+H]⁺ ion at $m/z = 147$ along with a major fragment at $m/z = 103$, indicating the characteristic fragmentation of its structure due to the loss of a CO group.

Our findings are consistent with earlier research demonstrating the abundance of these compounds in dill seeds. Umbelliferone, kaempferol, and quercetin were found in hydromethanolic extracts of dill seeds from Romania, according to Bota et al. [28]. Similarly, Mashraqi et al. [29] found that Saudi Arabian dill contained flavonoids and phenolic acids such as apigenin, quercetin, rosmarinic acid, caffeic acid, cinnamic acid, and chlorogenic acid. Along with these substances, Erdogan et al. [30] reported the abundance of rosmarinic acid and the existence of vanillic acid in Turkish seeds. Additionally, Meena et al.'s bibliographic study [31] revealed that dill seeds contain vitamins B1 and B2.

The literature has previously extensively reported the pharmacological characteristics of coumarins, particularly umbelliferone [32]. This coumarin has anti-inflammatory, antioxidant, antibacterial, antihyperglycemic, molluscicidal, and anticancer properties and is used as a sunscreen [33]. Because of their strong antioxidant activity, flavonoids

such as quercetin, kaempferol, and apigenin—which are renowned for their diverse pharmacological effects—are utilised as dietary supplements. Their broad variety of biological actions, including anti-inflammatory, antibacterial, anticancer, and cardioprotective effects, have been shown in several preclinical investigations [34–37].

Clinical studies have shown that phenolic acids are useful for a number of serious pathological conditions, such as viral infections, cancer, heart disease, hepatotoxicity, and neurotoxicity [38–41]. In addition to explaining the multiple pharmacological qualities of the dill seed extract that have been shown by the abovementioned investigations, the chemical composition of the extract also validates its use in traditional medicine. Supplementary Figure S4 shows the chemical structures of the main compounds present in *A. graveolens* seeds. Antioxidant Activity of Essential Oil and Extracts Essential Oil's Antioxidant Activity with DPPH The findings revealed a concentration-dependent variation in the *A. graveolens* essential oil's suppression of DPPH* radicals. Butylated hydroxytoluene (BHT) has a higher standard antioxidant capacity than Dill, based on the IC₅₀ values collected in Figure 4. In fact, the latter was thought to be less successful in lowering free radicals, with an IC₅₀ of 9.02 mg/mL.

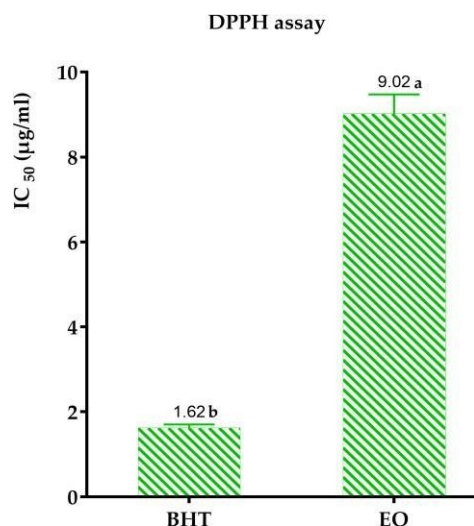


Figure 4. IC₅₀ values of *A. graveolens* and the standard antioxidant BHT using the DPPH method. The results with different letters are significantly different from each other ($p < 0.001$).

This finding has been documented in a number of earlier studies. In contrast to the typical ascorbic acid (IC₅₀ = 0.04 mg/mL), for example, Kauret al. [9] found using the DPPH technique that indole essential oil, which is mostly comprised of carvone (41.15%), limonene (23.11%), camphor (9.25%), and dihydrocarvone (3.75%), demonstrates modest antioxidant activity (IC₅₀ = 0.65 mg/mL). These scientists linked the existence of polar molecules to this antioxidant capacity. Similarly, using the DPPH technique, Osanloo et al. [42] found that Iranian dill essential oil has minimal antioxidant activity.

Its main ingredients are α -phellandrene (26.75%), p-cymene (24.81%), carvone (10.77%), dill ether (9.78%), and cis-sabinol (3.61%). According to a research done in Serbia, dill essential oil, which is mostly constituted of carvone (45.90%) and limonene (45.24%), has more antiradical action than anise, which is primarily formed of anethole (96.40%) [43]. Stanojević et al. [44] found that at a concentration of 29 mg/mL for 60 minutes, dill essential oil from Serbia, which is mostly constituted of carvone (85.9%), limonene (5.1%), and cis-dihydrocarvone (3.0%), inhibited 79.62% of DPPH

radicals.

The essential oil's antioxidant activity is established by the collective interaction of their chemical constituents, which may function in a synergistic or antagonistic manner. Because of their increased reactivity with peroxy radicals, essential oils that contain volatile phenolic components have strong antioxidant properties. Additionally, phenylpropanoids made up the majority of the EO of dill that we investigated (67.93%). Consequently, the antioxidant activity of phenylpropanoids has been observed in a number of earlier investigations [45]. Furthermore, the investigated EO, which was made up of fenchone (17.21%), estragole (29.32%), and trans-anethole (38.13%), shown mild antioxidant activity. Donati et al. has earlier recognised this poor antioxidant activity. [46]. Using the DPPH and FRAP methodologies, these researchers assessed the antioxidant activity of trans-anethole and estragole and discovered that they had a modest amount of antioxidant capacity. Furthermore, a different investigation by Senatore et al. [47] revealed that anethole's capacity to scavenge DPPH free radicals and lower ferric ions is inferior to that of the Trolox standard. Furthermore, Luís et al. [48] used the DPPH technique to investigate the antioxidant activity of *I. verum*'s essential oil, which is mostly constituted of phenylpropanoids (92.2%). The scientists discovered that this EO, rich in trans-anethole (88.5%), has an IC₅₀ (3.46%), which is almost 17 times greater than that of gallic acid (0.20%). As a result, this implies that *I. verum* EO's antioxidant capacity is much lower than that of

regular gallic acid. Furthermore, DPPH (1,1-diphenyl-2-picrylhydrazyl) experiments were used to investigate the antioxidant activity of Indian essential oil. Notably, the findings have shown modest antioxidant activity, with inhibition percentages for concentrations ranging from 5 to 25 μ L ranging from 26.1% to 43.62% [49]. Furthermore, using DPPH and ABTS techniques, Coêlho et al. [50] have shown the antioxidant potential of estragole; nevertheless, it is still less than that of Trolox. Using the FRAP technique, El Omari et al.'s study [51] has discovered that fenchone has a stronger reducing capacity than camphor and the essential oil of *Lavandula stoechas*. In a similar vein, Singhet al. [52] has emphasised fenchone's antioxidant properties. The moderate antioxidant activity of the studied dill EO is also attributed to the minor compounds, which may either strengthen or weaken its antioxidant activity through synergistic or antagonistic effects, even though these earlier studies have shown the antioxidant potential of trans-anethole, estragole, and fenchone. Extracts' Antioxidant Activity

The antioxidant properties of extracts from *A. graveolens* are shown based on the findings displayed in Figure 5. The IC₅₀ values for BHA and ascorbic acid were much lower than those of the extracts, which suggests that the standards had a high level of antioxidant activity. These compounds were employed as reference compounds by the DPPH and FRAP techniques.

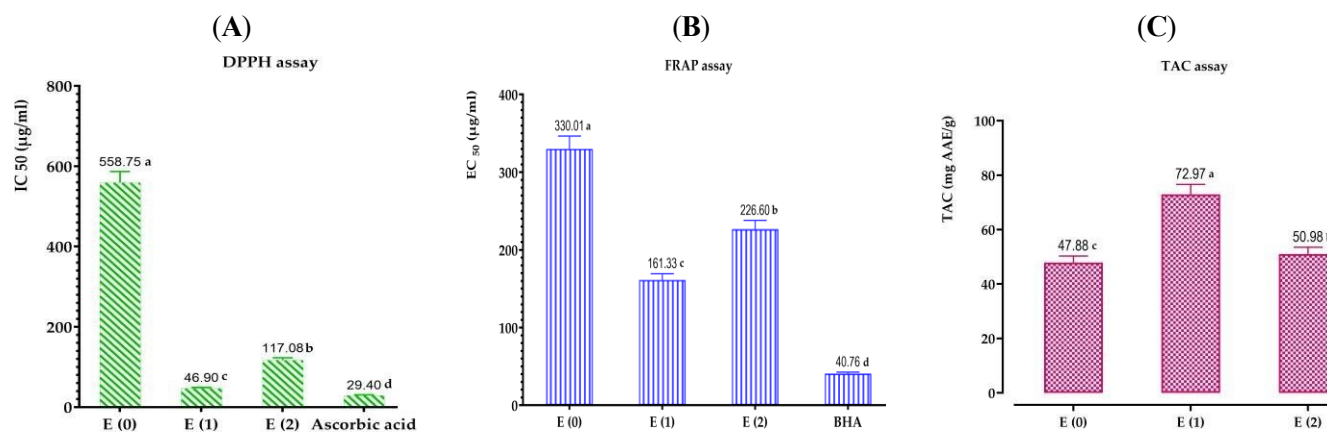


Figure 5. Antioxidant effects of extracts of *A. graveolens* by DPPH (A), and FRAP (B), and CAT (C). Mean values \pm standard deviations of determinations performed in triplicate are reported; Means are significantly different ($p < 0.001$).

Furthermore, we can see that the antioxidant activity is strongly influenced by the kind of extraction solvent used. Notably, the ethanolic extract has found to be the most active, with a robust antioxidant potential, in comparison to the aqueous extract and decoction. It has demonstrated high concentrations of polyphenols, flavonoids, and condensed tannins. Furthermore, every test has enabled us to demonstrate

that the ethanolic extract has stronger anti-radical ferric and molybdenum-reducing properties than the aqueous extract and decoction. In particular, the extract's IC₅₀ value is 46.90 ± 0.73 μ g/mL according to the DPPH technique, its EC₅₀ is 161.33 ± 6.18 μ g/mL according to the FRAP method, and its total antioxidant capacity is 72.97 ± 0.71 mg EAA/g E. Additionally, DPPH free radicals may be scavenged

more effectively by the aqueous extract than by the decoction. This is supported by the fact that the aqueous extract's IC₅₀ was lower (117.08±0.16 µg/mL) than the decoction's (IC₅₀ = 558.75± 4.07 µg/mL). Similarly, the aqueous extract showed a greater ability to decrease ferric and molybdenum ions than the decoction for the FRAP and TAC procedures; the EC₅₀ value was

The total antioxidant capacity was 50.98±0.2 mgEAA/gE, and the concentration was 226.60±11.73µg/mL. On the other hand, the decoction's total antioxidant capacity was 47.88 ± 1.73 mg EAA/g E, and its EC₅₀ was 330.01 ± 3.09 µg/mL. Furthermore, the presence of polyphenols, flavonoids, and other aromatic components is the main factor influencing the extracts' variation in antioxidant activity. We have found that the examined extracts contain significant amounts of phenolic compounds based on our examination of the phenolic compound test findings. The largest concentrations of polyphenols, flavonoids, and condensed tannins are found in the ethanolic extract, which surpasses both the aqueous extract and the often employed decoction in conventional medicine. We have also discovered a diverse chemical richness in the chemical profile of dill seeds, which is reflected by the presence of several chemical families like coumarins, flavonoids, phenolic acids, and terpenoids, thanks to the results of the chromatographic analyses

performed using HPLC/UV-ESI-MS for the decoction of dill seeds. Umbelliferone (12.35%), 3-hydroxyflavone (11.23%), rosmanol (8.95%), vitamin B7 biotin (8.36%), emmotin H (4.91%), and coumarin (4.21%) are its primary constituents. Several studies in the literature have confirmed the antioxidant properties of *A. graveolens* seeds. In particular, Basavegowda et al. Strong antioxidant properties of the methanolic extract of Indian dill seeds have been found [53]. Through the three radical scavenging techniques of DPPH, hydroxyl, and nitric oxide, they have shown IC₅₀ values of 19± 0.94, 28± 0.36, and 36± 0.64 µg/mL, respectively. Furthermore, Al-oqail et al. [16] have shown that the methanolic extract of sauidill seeds has a significant antioxidant capacity with IC₅₀ values of 225 and 126.3 µg/mL, respectively, using the DPPH and hydrogen peroxide scavenging techniques. Using the FRAP approach, these researchers have also discovered that at a concentration of 1 mg/mL, the extract's maximum absorbance is 1.387. El Mansouri et al.'s research [27] also shown the reducing power utilising FRAP and the antioxidant power of the aqueous extract of Morocco and dill seeds using the DPPH, ABTS, and hydroxyl radical scavenging techniques. Phenolic compound content and extracts' antioxidant activity are correlated.

All of the above findings demonstrate the connection between *A. graveolens*'s antioxidant activity and its phenolic components. The linear correlation coefficients were computed in light of this (Table 7).

Table 7. Correlation coefficients (R²) between polyphenol (PC), flavonoid (FC), tannin content (TC) and antioxidant activity of *A. graveolens* extract.

	PC	FC	TC	DPPH	FRAP	CAT
PC	1	0.907	0.994	0.970	0.990	0.762
FC	0.907	1	0.856	0.982	0.957	0.964
TC	0.994	0.856	1	0.938	0.969	0.969
DPPH	0.970	0.982	0.938	1	0.995	0.896
FRAP	0.990	0.957	0.969	0.995	1	0.845
CAT	0.762	0.964	0.686	0.896	0.845	1

The coefficients ranged from 0.686 to 0.990. Strong correlations were found between the extracts' total polyphenol content and the DPPH (R²=0.970), FRAP (R²=0.990), and CAT (R²=0.762) assays. Similarly, with Pearson coefficients of R² = 0.982, R² = 0.957, and R² = 0.964, respectively, a favourable association was found between the flavonoids and the anti-radical activity, reducing activity, and total antioxidant capacity. Their abundance of phenolic chemicals is responsible for the antioxidant action seen in our extracts. The exception is the condensed tannins, however. In the case of FRAP (R² = 0.969), DPPH (R²= 0.938), and CAT (R²= 0.686), there was a significant connection even though the ethanolic, aqueous, and decoction extracts did not have high amounts. This leads us to conclude that while the amount of condensed tannins is a significant component,

it is not always enough. When interpreting antioxidant power, another criteria pertaining to condensed tannins—the quality criterion—must be taken into account. A positive linear connection was also found between the three assessed antioxidant activities, as shown by the DPPH test and the CAT test (R² = 0.896), the DPPH test and the FRAP test (R² = 0.995), or the CAT test and the FRAP test (R² = 0.845). This discovery most likely suggests that the main chemicals involved in the anti-radical activity, reducing activity, and overall antioxidant capacity of the three extracts are polyphenols, flavonoids, and condensed tannins. Antimicrobial Activity The minimum bactericidal concentrations (MBCs), minimum fungicidal concentrations (MFCs), and minimum inhibitory concentrations (MICs) expressed in mg/mL for the

extracts and in $\mu\text{L}/\text{mL}$ for the essential oil of *Anethum graveolens* against the tested microorganisms are shown in Tables 8 and 9.

Table 8. MICs and MBCs (mg/mL) of *A. graveolens* EO and extracts (ethanolic, aqueous, and de-cocted).

Bacterial Strains	E (0)			E (1)			E (2)			EO		
	MIC	MBC	MBC/MIC	MIC	MBC	MBC/MIC	MIC	MBC	MBC/MIC	MIC	MBC	MBC/MIC
<i>E. cloacae</i>	50	50	1	>50	>50	-	50	50	1	25	25	1
<i>K. pneumoniae</i>	50	50	1	50	50	1	50	50	1	25	25	1
<i>E. coli</i>	>50	>50	-	>50	>50	-	>50	>50	-	25	25	1
<i>S. aureus</i>	50	50	1	50	50	1	50	50	1	25	50	2
<i>S. epidermidis</i>	>50	>50	-	>50	>50	-	>50	>50	-	50	50	1

Table 9. MIC and MFC of *A. graveolens* EO and extracts (ethanolic, aqueous, and decocted).

Fungal Strains	E (0)			E (1)			E (2)			EO		
	MIC	MFC	MFC/MIC	MIC	MFC	MFC/MIC	MIC	MFC	MFC/MIC	MIC	MFC	C
			C			C			C			
<i>C. albicans</i>	>50	>50	-	50	50	1	50	50	1	3.125	6.25	2
<i>C. dubliniensis</i>	>50	>50	-	6.25	6.25	1	12.5	12.5	1	3.125	3.125	1
<i>C. tropicalis</i>	>50	>50	-	12.5	12.5	1	25	25	1	6.25	6.25	1
<i>C. parapsilosis</i>	>50	>50	-	12.5	12.5	1	12.5	12.5	1	6.25	6.25	1
<i>A. niger</i>	>50	>50	-	0.78	0.78	1	25	25	1	3.125	3.125	1

With the exception of the decoction, which is inert, the data obtained indicate that the essential oil tested against the four fungus, dill extracts, has a potential antifungal activity. The MICs and MFCs for the ethanolic and aqueous extracts varied from 0.78 to 50 mg/mL. With MICs and MFCs of 0.78 mg/mL, *Aspergillus niger* was the most susceptible fungus. The highest MICs and MFCs measured against *Candida albicans* were 50 mg/mL. At the same dose of 12.5 mg/mL, the ethanolic and aqueous extracts demonstrated fungistatic and fungicidal activities on *C. parapsilosis*. Furthermore, we found that the ethanolic extract had a stronger antifungal effect than the other extracts that were evaluated. Its higher levels of flavonoids and polyphenols are directly responsible for this increased activity. The MICs and MFCs for the essential oil varied from 3.125 to 6.25 $\mu\text{L}/\text{mL}$. Notably, with MICs and MFCs of 3.13 $\mu\text{L}/\text{mL}$, the fungus *A. niger* and *C. dubliniensis* were the most sensitive. *Candida tropicalis* and *Candida parapsilosis* had the highest MICs and MFCs of 50 $\mu\text{L}/\text{mL}$.

The dill extracts and essential oil proved to be sensitive to different bacterial strains to differing degrees in terms of their antibacterial activities. In particular, the watery and

The decoction extracts shown bactericidal and bacteriostatic properties at 50 mg/mL on *K. pneumoniae* and *S. aureus*. Additionally, the ethanolic extract showed similar effects on all examined bacterial strains, with the exception of the *Enterobacter cloacae* strain, which showed no effect. Furthermore, none of the three studied extracts had any effect on *S. epidermidis* or wild-type *E. coli*. On the other hand, at a concentration of 25 $\mu\text{L}/\text{mL}$, the essential oil inhibited and killed wild-type *E. coli* bacteria, *K. pneumoniae*, and *E. cloacae*. In contrast, *S. aureus* and *S. epidermidis* showed higher MBCs of 50 $\mu\text{L}/\text{mL}$, suggesting that they were less susceptible. These findings support those of Kaur et al. [54]. With MICs of 40 and 20 mg/mL, respectively, these authors have highlighted the antibacterial activity of the aqueous extract of Indian and dill seeds against *E. coli* and *S. aureus*. The antibacterial efficacy of essential oils derived from various components, including the leaves, stems, flowers, and seeds of *A. graveolens* from Saudi Arabia, has also been shown by another research. Additionally, this research showed that the seeds' essential oil, which is made up of dillapiole (33.3%), limonene (30.8%), carvone (17.7%), and trans-dihydrocarvone (12.2%), had a stronger antimicrobial effect than the essential oils from the other components against *S. aureus*, *C. albicans*, and *C. parapsilosis* [25]. The methanolic extract of Indian dill seeds has been shown to exhibit

antibacterial properties against *E. coli*, *K. pneumoniae*, and *S. aureus*, with MICs of 1250, 833, and 125 $\mu\text{g/mL}$, respectively, according to Basavegowda et al. [53]. In general, the essential oil's chemical makeup is directly related to its demonstrated antimicrobial activity. Furthermore, the unique antibacterial properties of the essential oil of *Foeniculum vulgare* seeds have been ascribed by Mota et al. [55] to the combined action of the main constituents, which are present in an equal proportion and are (E)-anethole (37.2%), estragole (31.1%), and fenchone (28.5%). Thus, the three primary compounds in our study's essential oil analysis were (E)-anethole (38.13%), estragole (29.32%), and fenchone (17.21%), all of which were present in about equal percentages. As a result, the antibacterial action may be ascribed to the synergistic effects of the main components in this complex combination. Additionally, the presence of ketones (17.57%) and the richness of the examined essential oil in ethers (68.04%) might both be linked to the observed antibacterial capability. Assessment of Potentially Active Compounds Isolated from the Essential Oil and Aqueous Extract of *A. graveolens* Seeds for PASS Activity, ADME, Toxicity (ProTox II), and Efficacy In addition to its biological attributes, evaluating the physicochemical characteristics of the candidate compounds is essential for creating therapeutic agents and verifying *A. graveolens*' efficacy as a nutraceutical preservative agent. To ascertain the pharmacokinetic and physicochemical properties of the compounds included in the essential oil and aqueous extract of *A. graveolens* seeds, as well as their resemblance to pharmaceuticals, an analysis was carried out. The aqueous extract (umbelliferone, 3-hydroxyflavone, rosmanol, biotin, emmotin, coumarin, trans-caftaric acid, pimelic acid, methylrosmarinate, homovanillic acid, 1-caffeoyl-beta-D-glucose, and kaempferol) and the EO (E)-anethole, estragole, fenchone, and α -pinene) of *A. graveolens* were chosen for PASS and ADMET (absorption, distribution, metabolism, excretion, and toxicity) prediction studies. The SwissADME and pkCSM [58] online tools, the PASS webprediction tool [57], and the ChemBio-Draw webtool [56] were used to produce the SMILES representations of these compounds. Table 10 displays the results of the PASS and ADMET prediction experiments. PASS predictions were used to assess the effectiveness of the antioxidant and antibacterial qualities of the main constituents isolated from the EO and aqueous extract of *A. graveolens* seeds. All of the significant compounds exhibited significant "Pa" values for several activities, including antioxidant (0.150–0.856), antifungal (0.267–0.717), and antibacterial potential (0.216–0.587), according to our estimates (Table 10). Additionally, these substances had extremely good antioxidant properties, strong antifungal

effects, and strong antibacterial properties. The SwissADME and PkCSM websites are helpful for examining the pharmacokinetic characteristics and how closely a chemical resembles a medication. All of the chosen compounds' lipophilicity indices show that they are very soluble in water (Table 10). The selected materials exhibit high Caco-2 permeability values and favourable skin permeability (log Kp) values. With the exception of trans-caftaric acid, the majority of the substances under study exhibit good intestinal absorption (HIA > 30%). P-glycoprotein, often known as P-gp, is essential for the distribution and absorption of medications. The primary components of the essential oil are also not P-gp substrates, and none of the chemical compounds from the study behave as inhibitors of P-gpI and P-gpII. By contrast, we found that molecules such as 3-hydroxyflavone, rosmanol, methyl rosmarinate, homovanillic acid, 1-caffeoyl-beta-D-glucose, and kaempferol may be P-gp substrates in the aqueous extract. Furthermore, the only substance that could inhibit P-gp I was rosmanol. Eight of the sixteen isolated compounds that were examined had an SNC score higher than -3.0, indicating that they are likely to pass across the blood-brain barrier (BBB) with ease. Nevertheless, few exceptions were observed, especially for 1-caffeoyl-beta-D-glucose, biotin, emmotin H, coumarin, trans-caftaric acid, pimelic acid, methylrosmarinate, and homovanillic acid, which did not meet this threshold. We identified the chemicals from the examined essential oils and 3-hydroxyflavone from the watery extract as having limited penetration into the central nervous system (log BB > 0.3). From -1.533 L/kg to 1.274 L/kg, their volume of distribution in tissues (log VDss) varied. Although the primary components of the essential oil and the analysed aqueous extract are unlikely to have adverse effects when taken orally owing to drug interactions, cytochrome P450 (CYP) enzymes and molecular interactions are key in the removal of pharmaceuticals. To forecast the excretion route, the total clearance of hepatic and renal substrates (CLTOT) and the retinal organic cation transporters 2 (OCT2) were expressed in log mL/min/kg. According to the statistics, every phytochemical component under study had excellent overall clearance values and was eliminated. Several factors, including AMES, hERG channel inhibition, skin sensitisation, immunotoxicity, hepatotoxicity, carcinogenicity, mutagenicity, and cytotoxicity, were investigated in order to assess the possibly detrimental effects of the essential oil and aqueous extract of *A. graveolens* seeds. The primary phytochemical components were the focus of the study, as shown in Table 11. With the exception of certain compounds, the results showed no discernible harmful consequences. (E)-anethole, estragole, umbelliferone, 3-hydroxyflavone, and coumarin may have minor

carcinogenic effects; biotin may have mild liver effects. Nevertheless, 1-Caffeoyl-beta-D-glucose, methyl rosmarinate, trans-caftaric acid, and rosmanol may exhibit immunotoxic effects. Lastly, umbelliferone, often referred to as 7-hydroxycoumarin, is a naturally occurring chemical molecule that is widely dispersed throughout the coumarin family. It is classed in the anticipated toxicity class 6 and has an LD50 of 10,000 mg/kg. One of the primary components of the aqueous extract of the *A. graveolens* seeds under study is this chemical. These results show that the essential oil and aqueous extracts made from southern Moroccan *A. graveolens* seeds may be regarded as safe for oral use as nutraceuticals and/or as natural alternatives to artificial preservatives, provided that the recommended dosages are adhered to. However, to definitively confirm that there are no long-term hazards to consumers

Fraction unbound (human)	bound (human)	0.266	0.213	0.423	0.425	0.432	0.151	0.109	0.58	0.3	0.367	0.472	0.543	0.229	0.467	0.609	0.178
	BBB permeability	0.529	0.601	0.624	0.791	-0.278	0.462	-0.581	-0.679	0.291	-0.007	-1.233	-0.21	-1.454	-0.312	-1.081	-0.939
	CNS permeability	-1.659	-1.74	-1.988	-2.201	-2.741	-1.733	-2.101	-3.541	-2.784	-1.926	-3.93	-3.042	-3.358	-2.723	-3.982	-2.228
Metabolism Parameters Prediction	CYP2D6 substrate	No	No	No	No	No	No	No	No	No	No	No	No	No	No	No	No
	CYP3A4 substrate	No	No	No	No	No	Yes	No	No	No	No	No	No	Yes	No	No	No
	CYP1A2 inhibitor	Yes	Yes	No	No	Yes	Yes	No	No	Yes	Yes	No	No	No	No	No	Yes
	CYP2C19 inhibitor	No	No	No	No	No	Yes	No	No	No	No	No	No	No	No	No	No
	CYP2C9 inhibitor	No	No	No	No	No	No	No	No	No	No	No	No	No	No	No	No
	CYP2D6 inhibitor	No	No	No	No	No	No	No	No	No	No	No	No	No	No	No	No
	CYP3A4 inhibitor	No	No	No	No	No	No	No	No	No	No	No	No	No	No	No	No
Excretion	Total Clearance	0.268	0.332	0.085	0.043	0.706	0.233	0.289	0.368	0.19	0.97	0.449	0.565	0.187	0.246	0.059	0.477
	Renal Clearance	No	No	No	No	No	No	No	No	No	No	No	No	No	No	No	No

EO1: E-Anethole; EO2: Estragole; EO3: Fenchone; EO4: α -Pinene; D1: Umbelliferone; D2: 3-hydroxyflavone; D3: Rosmanol; D4: Biotine; D5: EmmotinH; D6: Coumarin; D7: trans-Caftaric acid; D8: pimelic acid; D9: Methyl rosmarinate; D10: Homovanillic Acid; D11: 1-Caffeoyl-beta-D-glucose; D12: Kaempferol.

Table 11. Insilico analysis of the predictive toxicity (ProToxII) of Compounds from the Essential Oil and Decoction of *A. graveolens* Seeds.

Compounds	AMES Toxicity	hERG I Inhibitor	hERGI Inhibitor	Skin Sensitization	Minnow LD ₅₀ Toxicity (mg/kg)	Predicted Toxicity Class	Hepatotoxicity	Carcinogenicity	Immunotoxicity	Mutagenicity	Cytotoxicity
EO1	No	Yes			0.869	150	3		Active(0.57)		
EO2	Yes		No	Yes	1.398	1230	4	Inactive	Active(0.51)		
EO3	No			Yes	1.366	775	4		Inactive		Inactive
EO4	No			No	1.159	3700	5		Inactive		
D1	No		No		1.714	10,000	6	Inactive	Active(0.64)	Inactive	Inactive
D2	Yes		No		1.205	2500	5	Inactive	Inactive	Inactive	Inactive
D3	No		Yes		0.285	450	4	Inactive	Inactive	Active(0.95)	Inactive
D4	No		No		2.183	4000	5	Active(0.41)	Inactive	Inactive	Inactive
D5	No		No		1.329	1600	4	Inactive	Inactive	Inactive	Inactive
D6	No		No		1.555	196	3	Inactive	Active(0.83)	Inactive	Active(0.55)
D7	No	No	No	No		3800	5	Inactive	Inactive	Active(0.97)	Inactive
D8	No		No	2.006		900	4	Inactive	Inactive	Inactive	Inactive
D9	No		No	1.92		5000	5	Inactive	Inactive	Active(0.93)	Inactive
D10	No		No	2.106		1123	4	Inactive	Inactive	Inactive	Inactive
D11	No		No	5.989		5000	5	Inactive	Inactive	Active(0.95)	Inactive
D12	No		No	2.885		3919	5	Inactive	Inactive	Inactive	Inactive

EO1: E-Anethole; EO2: Estragole; EO3: Fenchone; EO4: α -Pinene; D1: Umbelliferone; D2: 3-hydroxyflavone; D3: Rosmanol; D4: Biotine; D5: EmmotinH; D6: Coumarin; D7: trans-Caftaric acid; D8: pimelic acid; D9: Methyl rosmarinat; D10: Homovanillic Acid; D11: 1-Caffeoyl-beta-D-glucose; D12: Kaempferol.

Molecular Docking

The chemicals identified using GC/MS and HPLC/UV-ESI-MS were selected for *in silico* molecular docking investigations in light of the much higher *in vitro* bioactivities shown in the EO and aqueous extract of *A. graveolens* in this study. Molecular docking experiments were used to determine the compounds' antibacterial, antifungal, and antioxidant properties as well as their possible mode of action. The chemical interactions between the compounds and their respective target proteins (1JZQ, 1KZN, 2CAG, 2VEG, 2ZDQ, 3SRW, 3UDI, 4URN, 2CDU, 1OG5, and 3NRZ) at the atomic level served as the basis for these conclusions. The majority of the molecular docking research was focused on evaluating elements like hydrogen bonds, Van der Waals (VDW) interactions, binding free energy, and carbon–hydrogen (C–H) bonds. While hydrogen bonds and VanderWaals (VDW) interactions affect the binding interactions, C-H bonds and Pi-sigma interactions regulate the stability of the ligands (selected molecules) and the docked receptor. The docking energy binding scores for the binding sites of the target proteins implicated in antioxidant activities (2CDU, 1OG5, and 3NRZ) and antibacterial activities (1JZQ, 1KZN, 2CAG, 2VEG, 2ZDQ, 3SRW, 3UDI, and 4URN) are shown in Table 12. The Van der Waals interactions, hydrogen bonds, and C-H bonds involving the amino acids present in the binding sites of the chosen proteins were examined in this work.

Ligands\Targets	1JZQ	1KZN	2CAG	2VEG	2ZDQ	3SRW	3UDI	4URN	2CDU	1OG5	3NRZ
EO1	-5.1	-5.6	-7.1	-4.8	-7.1	-5.8	-4.7	-5.5	-5.6	-5.4	-7.5
EO2	-5.2	-5.6	-6.7	-4.5	-7.0	-5.5	-4.6	-5.3	-5.5	-5.3	-7.0
EO3	-5.6	-4.8	-6.5	-4.6	-6.6	-5.9	-5.0	-4.7	-5.3	-6.0	-6.2
EO4	-5.5	-4.6	-6.0	-4.6	-6.2	-5.6	-4.5	-4.6	-5.0	-5.5	-5.1
D1	-6.0	-6.7	-8.1	-5.8	-8.2	-6.4	-5.8	-6.2	-6.4	-6.3	-8.8
D2	-7.6	-7.7	-9.4	-7.0	-8.4	-8.1	-7.4	-7.5	-7.5	-7.9	-8.8
D3	-8.2	-8.0	-7.2	-7.0	-6.5	-8.6	-8.2	-7.7	-7.3	-8.9	-6.2
D4	-6.3	-6.2	-7.5	-5.3	-7.3	-7.0	-6.0	-6.2	-6.1	-7.1	-7.0
D5	-7.5	-7.5	-9.0	-6.2	-10.0	-8.0	-7.6	-6.3	-7.6	-8.0	-6.2
D6	-5.8	-6.6	-7.7	-5.5	-7.9	-6.3	-5.6	-5.8	-6.4	-6.6	-8.1
D7	-6.8	-7.3	-8.9	-6.8	-9.1	-7.8	-7.2	-6.5	-7.9	-7.3	-7.6
D8	-4.9	-5.2	-5.9	-4.5	-5.8	-4.9	-4.9	-4.9	-5.1	-5.4	-6.6
D9	-7.8	-8.4	-10.2	-7.8	-9.2	-8.4	-8.3	-7.3	-8.0	-8.4	-9.8
D10	-5.5	-6.1	-7.1	-5.4	-7.0	-6.0	-5.5	-5.5	-6.1	-6.0	-7.4
D11	-7.6	-7.6	-9.5	-6.7	-9.8	-8.0	-7.4	-7.0	-7.7	-7.9	-10.0
D12	-8.1	-8.2	-10.0	-6.6	-9.0	-8.5	-8.3	-7.9	-7.7	-8.6	-7.8

Table 12.

It should be noted that a protein target may experience substantial conformational changes when interacting with a pharmacological molecule. A useful technique for comprehending the internal movements, conformational changes, and stability of protein–ligand complexes is molecular dynamics simulation (MDS). By analysing MD trajectories for the ten complexes—two in the case of 3NRZ, four in the case of 2CAG, and four in the case of 2ZDQ—parameters like root-mean-square deviation (RMSD), root-mean-square fluctuation (RMSF), radius of gyration (Rg), number of hydrogen bonds, and binding free energy can be calculated. These investigations provide light on the complexes' binding strengths, mechanisms, and structural stability.

3NRZ's Structural Dynamics
The intricate structural dynamics of protein 3NRZ in interaction with methyl-rosmarite and 1-caffeoyl-beta-D-glucose ligands were examined in our work using molecular dynamics simulations. Our goal was to comprehend the minute impacts that ligand binding has on the protein's conformational stability. To understand the dynamic interaction between the protein and ligands, we focused on a number of metrics. It is evident from looking at the RMSD graph in Figure 12 that all of the protein-ligand entities had less spectrum variation. This suggests that their structural dynamics were only slightly disturbed over the full simulation. The RMSF analysis examined the effects of ligand binding on protein dynamics over 100 ns, finding that protein–ligand complexes had less flexibility and a reduced capacity for conformational alterations. This implies that all complexes, as shown in Figure 12, have little effect on receptor flexibility. Additionally, analysis of the Radius of Gyration (RG) profiles showed steady patterns in both complexes, indicating that a stable configuration was maintained. The development of numerous hydrogen bonds in both complexes was shown by hydrogen bonding analysis, which highlights the crucial role that these bonds play in maintaining stability even when ligands dissociate.

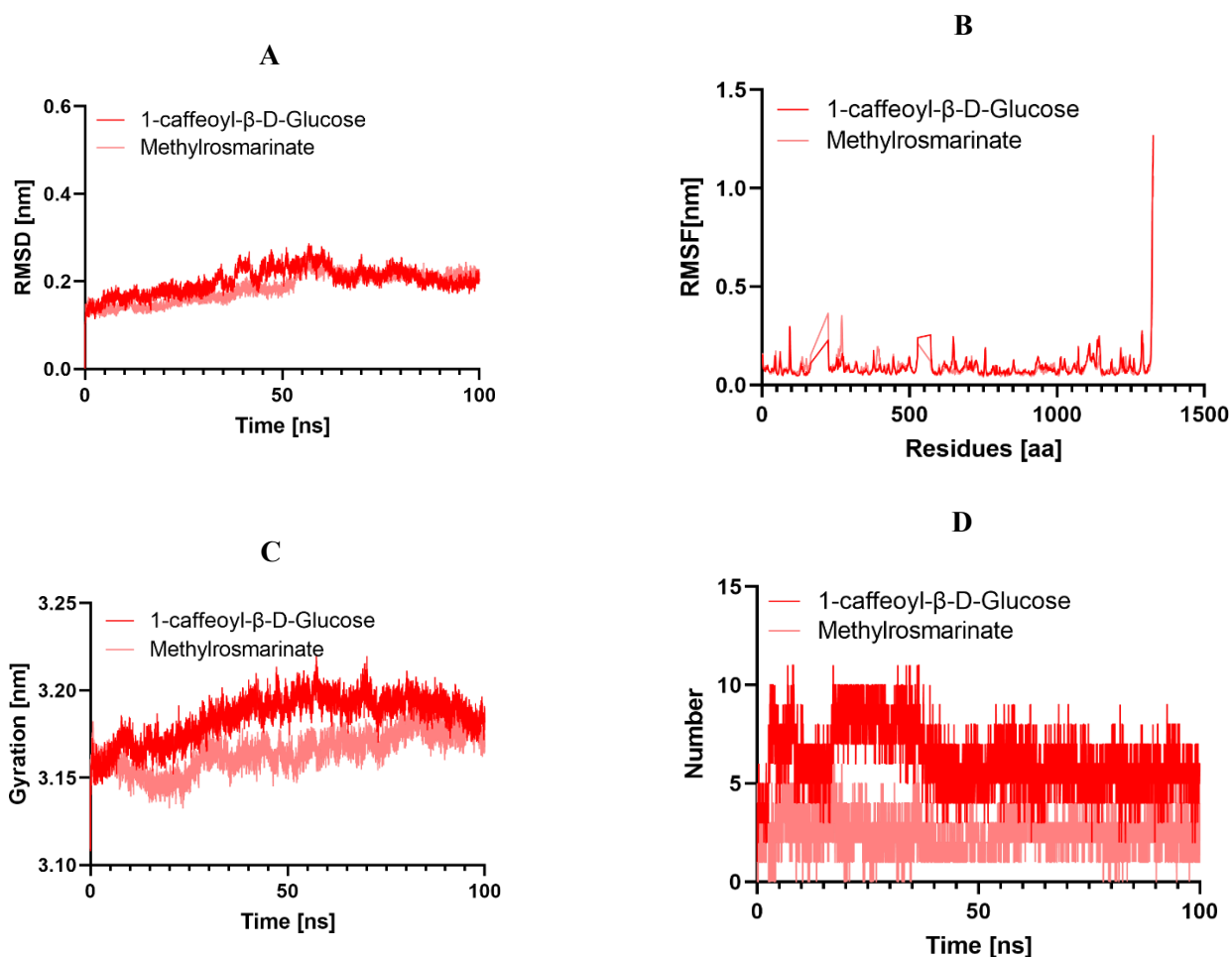


Figure 12. Structural dynamics of the 3NRZ protein: (A) RMSD and (B) RMSF. (C) Total number of intramolecular hydrogen bonds. (D) Radius of gyration.

Structural Dynamics of 2CAG

Using molecular dynamics simulations, we investigated the structural dynamics of 2CAG in this work, concentrating on how they interacted with different ligands (Figure 13). Our investigation revealed the effects of four distinct ligands on protein conformation and dynamics: 3-hydroxyflavone, methylrosmarinate, 1-caffeoyl-β-D-glucose, and kaempferol. With the exception of kaempferol, which showed a noticeably greater RMSD, we found very identical RMSD patterns throughout the protein-ligand complexes, suggesting minor conformational changes following ligand binding. This implies that whereas 3-hydroxyflavone, methylrosmarinate, and 1-caffeoyl-β-D-glucose create small structural changes in the protein backbone, kaempferol causes more noticeable alterations, which may indicate a different binding mechanism or affinity. The complexes 2CAG/3-hydroxyflavone, 2CAG/Methylrosmarinate, and 2CAG/1-caffeoyl-β-D-glucose showed similar dynamics, according to further examination of RMSF patterns. However, the 2CAG/Kaempferol complex showed increased flexibility, suggesting that the ligands had varied effects

on protein flexibility. Using the radius of gyration (R_g) to examine protein compactness, 3-hydroxyflavone, methylrosmarinate, and 1-caffeoyl-β-D-glucose were shown to have greater protein compactness than Kaempferol, indicating tighter protein structure binding and corresponding with the RMSD findings. Furthermore, simulations revealed that 3-hydroxyflavone, methylrosmarinate, and 1-caffeoyl-β-D-glucose the target proteins formed hydrogen bonds during a 100 ns period, indicating significant molecular interactions that support sustained binding. Kaempferol, on the other hand, generated fewer hydrogen bonds, suggesting less effective or advantageous interactions with the protein.

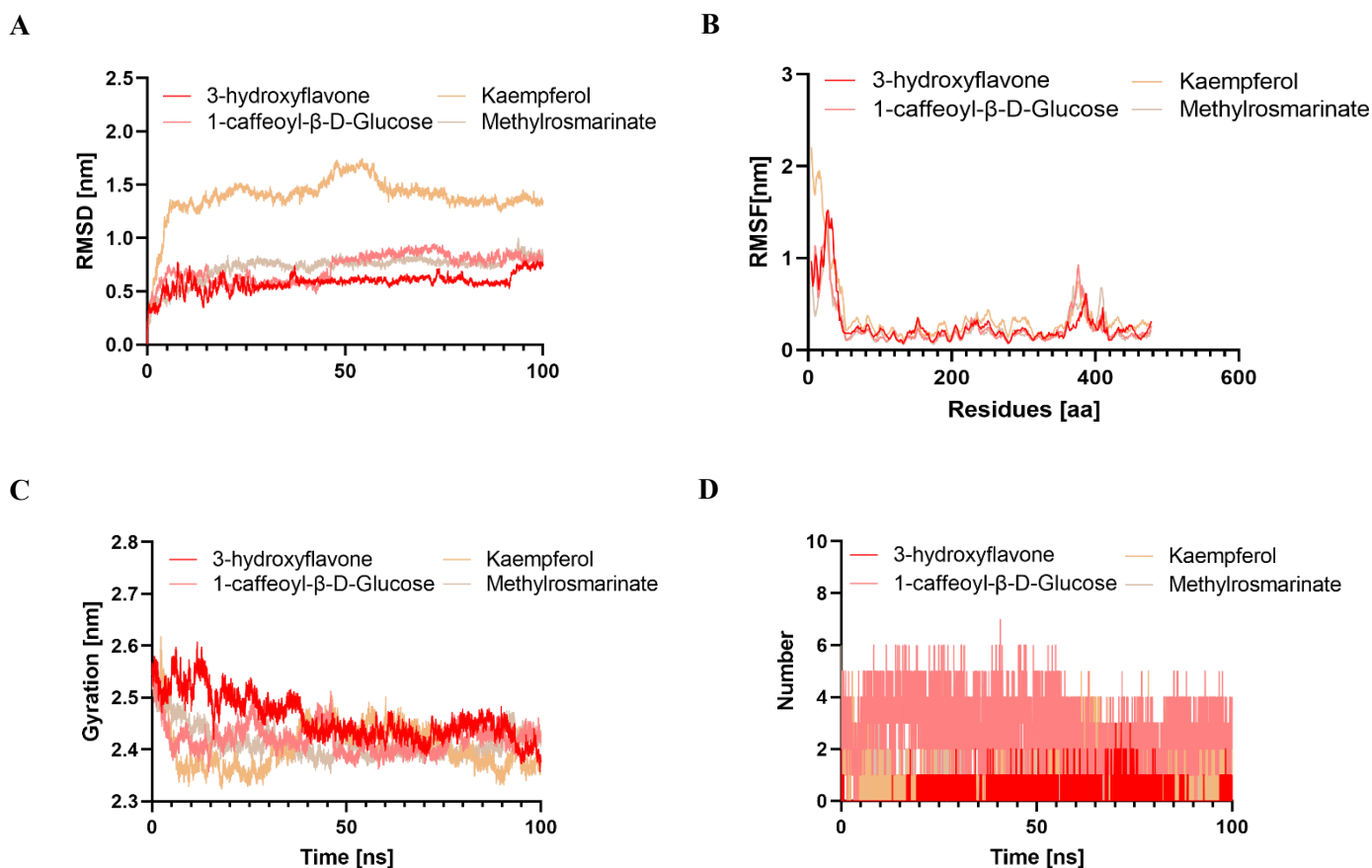


Figure 13. Structural dynamics of the 2CAG protein: (A) RMSD and (B) RMSF. (C) Total number of intramolecular hydrogen bonds. (D) Radius of gyration.

Structural Dynamics of 2ZDQ

In this instance, we used molecular dynamics simulations to investigate the structural dynamics of 2ZDQ, concentrating on its interactions with four different ligands: emmotin H, trans-caftaric acid, methylrosmarinate, and 1-caffeoyl-β-D-glucose. This study provides insight into their impact on protein dynamics and structure. With the exception of emmotin H, which showed a noticeably greater RMSD, we found very identical RMSD patterns throughout the protein-ligand complexes, suggesting minor conformational changes following ligand binding. This implies that emmotin H causes more noticeable alterations in the protein backbone, perhaps indicating a different binding mechanism or affinity, while trans-caftaric acid, methylrosmarinate, and 1-caffeoyl-β-D-glucose cause insignificant structural rearrangements. Complexes produced with trans-caftaric acid, methylrosmarinate, or 1-caffeoyl-β-D-glucose exhibited comparable kinetics, according to further study of RMSF patterns. Nonetheless, the emmotin H-2ZDQ complex had

enhanced flexibility, indicating that the ligands had varying impacts on the protein's flexibility. We then investigated the modifications to the protein's structural compactness brought about by its interactions with these different substances. We calculated the radius of gyration (Rg) over time in order to do this (Figure 14). In accordance with the findings of the protein backbone's RMSD analysis, the protein compactness analysis Trans-caftaric acid, methylrosmarinate, and 1-caffeoyl-β-D-glucose were shown to increase protein compactness in comparison to emmotin H utilising the Rg. Additionally, simulations demonstrated the formation of hydrogen bonds between the target protein and trans-caftaric acid, methylrosmarinate, or 1-caffeoyl-β-D-glucose during a 100 ns time span, suggesting significant molecular interactions favourable for long-term binding. Emmotin H, on the other hand, formed fewer hydrogen bonds, indicating that its interactions with the protein were less beneficial or weaker.

A

B

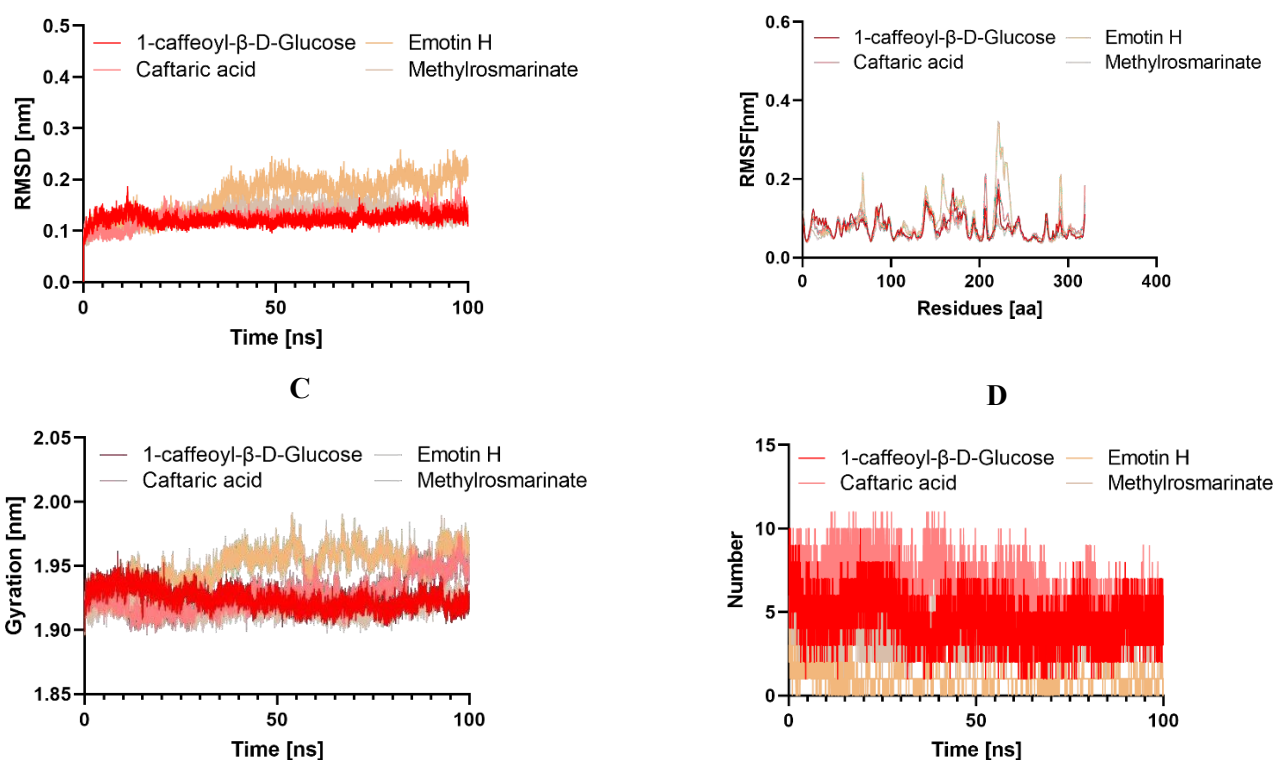


Figure 14. Structural dynamics of the 2ZDQ protein: (A) RMSD and (B) RMSF. (C) Total number of intramolecular hydrogen bonds. (D) Radius of gyration.

It is crucial to examine in detail the physico-chemical characteristics of potential compounds, as well as the pharmacokinetic and physicochemical properties of the substances identified in the essential oil (EO) and aqueous extract (E0) of *A. graveolens* seeds, comparing them to drugs, in order to design therapeutic agents and support the efficacy of the chemical composition of *A. graveolens* as a nutraceutical preservative. Significant results were found for a number of activities, including antioxidant, antifungal, and antibacterial qualities, according to the predictive PASS and AD-MET assessment of the primary components of the EO and aqueous extract (AE) of *A. graveolens*. The antioxidant and antibacterial properties of the chemicals found in *A. graveolens* have been confirmed by earlier research, especially that of Najaranetal [59], Noumietal [23], and Madhuri [60], indicating their potential as therapeutic agents for a variety of illnesses. These results demonstrate the remarkable properties of the compounds found in the EO and aqueous extract (E0) of *A. graveolens*, which show significant antibacterial, antifungal, and antioxidant properties.

There are several pharmacological and biological uses for the primary phenolic, flavonoid, and terpenoid chemicals that are isolated from *A. graveolens* seeds. In preclinical research, these compounds show encouraging antibacterial, antioxidant, and anticancer qualities. The

biological action of these compounds, which include methyl rosmarinate, trans-caftaric acid, 1-caffeoyl-beta-D-glucose, kaempferol, and 3-hydroxyflavone, is now being investigated. Methyl rosmarinate is notable for its antifungal and antioxidative qualities. It has inhibitory properties against matrix metalloproteinase-1 (MMP-1), α -glucosidase, and tyrosinase [61–64]. In addition to its neuroprotective properties, trans-caffeic acid has potential as an antioxidant, anti-inflammatory, antimutagenic, anticarcinogenic, hepatoprotective, antidiabetic, antihypertensive, anti-obesity, and metabolic syndrome [65]. 1. A number of pharmacological actions are shown by caffeineyl-beta-D-glucose, kaempferol, and 3-hydroxyflavone, indicating a substantial involvement in a number of therapeutic fields [66,67].

Our molecular docking studies show important interactions between a number of bioactive substances and different target proteins that have antibacterial and antioxidant properties. The chemicals that showed the highest binding energies with the proteins under investigation were 3-hydroxyflavone, emmotin H, trans-caftaric acid, methyl rosmarinate, 1-caffeoyl-beta-D-glucose, and kaempferol. These substances have shown a high affinity for certain proteins, including 2CAG, 2ZDQ, and 3NRZ, suggesting that they may have antibacterial and antioxidant properties. Additionally, the investigation of molecular interactions with certain

catalase residues using 3-hydroxyflavone showed hydrogen bonds, Pi-alkyl bonds, Pi-cation contacts, and Pi-Pi-shaped interactions. Similarly, trans-caftaric acid created hydrogen bonds and Pi-Pi stacking with the residues of D-Alanine Ligase, whereas emmotin formed hydrogen bonds, Pi-Pi stacking, and Pi-alkyl interactions with the latter residues. These particular interactions demonstrate the variety of ways that the bioactive chemicals interact with the target proteins. Additionally, the existence of hydrogen bonds, carbon-hydrogen bonds, Pi-Pi stacking contacts, and Pi-alkyl interactions was discovered by the examination of catalytic residues in interactions with methylomarinate. Furthermore, this molecule's interactions with D-Alanine ligase were described via Pi-cation interactions, Pi-anion contacts, Pi-Pi stacking interactions, hydrogen bonds, and carbon-hydrogen bonds. Hydrogen bonds, carbon-hydrogen bonds, Pi-Pi stacked contacts, Pi-Pi-shaped interactions, and Pi-alkyl interactions were finally seen in interactions with 3NRZ. Numerous connections, including hydrogen bonds, carbon-hydrogen bonds, Pi-sigma contacts, Pi-Pi stacking interactions, and Pi-alkyl interactions, were linked to 1-Caffeoyl-beta-D-glucose's interactions with catalase, D-Alanine ligase, and bovinexanthineoxidase. Additionally, the stability of protein-ligand complexes and conformational changes were revealed by the investigation of structural dynamics using molecular dynamics simulations [68]. These simulations showed both notable variances and comparable dynamic behaviours across several complexes, indicating different interaction modalities and varying implications on the stability and flexibility of proteins. These findings open up new avenues for study in the domains of natural products and pharmaceutical chemistry by highlighting the variety of molecular interactions that exist between bioactive substances and target proteins. In the end, these chemicals still require FDA clearance for medical usage despite their great therapeutic potential. This emphasises the need for further study, especially clinical trials, to determine their safety and

effectiveness in treating oxidative stress in patients. By regulating the production of certain cytokines and enzymes like SOD, dehydrase, CAT, GST, GSH, GPx, and GRd, these molecules are being investigated for their antioxidant capacity and may function as scavengers of pharmaceuticals, protecting cells from oxidative stress-induced ageing. The results of molecular docking studies may help to clarify the antioxidant activity of *A. graveolens* essential oil, which was assessed using the DPPH approach and valued at an IC₅₀ of 9.02 mg/mL. Therefore, substances like fenchone and trans-anethole, which have shown strong interactions with certain proteins linked to antioxidant processes like catalases or superoxide dismutases, can be responsible for the observed antiradical activity in lab settings. These compounds have excellent structural and electrical properties that help neutralise free radicals. This is mostly because of their terpenic or phenolic groups, which have the ability to effectively eliminate reactive oxygen species. Minimum inhibitory concentrations (MICs) and minimum bactericidal concentrations (MBCs) for the extracts' and essential oils' antifungal and antibacterial properties ranged from 0.78 to 50 mg/mL and 3.125 to 6.25 µL/mL, respectively. Molecular docking studies have discovered binding energies and interactions, including hydrogen bonding and Van der Waals forces, that are responsible for these activities. The powerful bond between emmotin H, a phenolic compound present in the

The proteins 2ZDQ and 2CAG, which are essential enzymes in bacteria and fungus, and the hydro-ethanolic extract may be responsible for the extract's strong antibacterial activity against *Aspergillus niger* and *Candida albicans*. Emmotin and these proteins had binding energies of -10 and -9.4 kcal/mol, respectively. Without a doubt, this kind of selective molecular interaction is likely to disrupt the general structure and functional stability of these particular proteins, which will restrict the growth of microorganisms and their metabolic activities.

3. Materials and Methods

Plant Material

Anethum graveolens belongs to the *Apiaceae* family, commonly known as dill. The sample under study was collected from a cultivated population in the Errachidia area. Table 13 provides information on the collection location, the component harvested, and the origin. This species was identified at the Laboratory of Botany and Plant Ecology of the Scientific Institute of Rabat, Department of Botany.

Table 13. Harvesting Site, Parts Used, Habitat, and Harvesting Season for *A. graveolens*.

Scientific Name	Part Collected	Harvesting Area				Harvest Period	
		Region	Location	Latitude(x)	Longitude (y)		Altitude(m)
<i>Anethum graveolens</i>	Seeds	Errachidia	Annif	31°06'54"N	5°09'38"W	905	June 2022

Microbiological Materials

In this study, the antimicrobial activity of the essential oil (EO) and extracts of *A. graveolens* seeds was evaluated against five bacterial and five fungal strains. These microorganisms are pathogens commonly encountered in various human diseases (Table 14). These strains were isolated from the hospital environment of the Mohamed V Provincial Hospital, Meknes. All strains were stored in a 20% glycerol stock at -80°C, rejuvenated in Mueller–Hinton and Sabouraud broths, and subcultured before use.

Table 14. List of tested bacterial and fungal strains used for antimicrobial tests.

		Strains	Abbreviations
Bacteria	Gram-negative bacilli	<i>Enterobacter cloacae</i>	<i>E. cloacae</i>
		<i>Klebsiella pneumoniae</i>	<i>K. pneumoniae</i>
Gram-positive cocci		<i>Escherichia coli</i>	<i>E. coli</i>
		<i>Staphylococcus aureus</i>	<i>S. aureus</i>
		<i>Staphylococcus epidermidis</i>	<i>S. epidermidis</i>
Yeasts	Fungi	<i>Candida albicans</i>	<i>C. albicans</i>
		<i>Candida dubliniensis</i>	<i>C. dubliniensis</i>
		<i>Candida tropicalis</i>	<i>C. tropicalis</i>
		<i>Candida parapsilosis</i>	<i>C. parapsilosis</i>
	Mold	<i>Aspergillus niger</i>	<i>A. niger</i>

Quality Control of Plant Material

Moisture Content

The approach used to determine the moisture content complied with the AFNOR standard (NF-V03-4021985) [69]. A total of 5 g of plant samples were measured using pre-dried and pre-weighed crucibles. The crucibles, which held the plant material, were thereafter placed in an oven and exposed to a temperature ranging from 103 to 105 °C for a duration of 24 h. Subsequently, the samples were subjected to cooling in a desiccator and

subsequently weighed. The moisture content was calculated using the formula (1). The experiment was repeated three times.

$$MC\% = \left(\frac{m_0 - m_1}{m_0} \right) \times 100$$

With m_0 as the initial mass of the plant in (g) and m_1 as the mass after drying in (g). The result is expressed as a percentage of dry matter.

Ash Content

The ash content refers to the amount of mineral materials that remain after the organic matter was destroyed by high-temperature incineration in a furnace. A total of 5 g of ground samples were put in a muffle furnace at a temperature of 550°C until all charred particles were destroyed and whitish ashes were obtained, which had a consistent weight (according to NFISO 5984) [70]. The organic matter content was determined by employing the subsequent formula (2):

$$OM\% = \left(\frac{m_1 - m_2}{TE} \right) \times 100 \quad (2)$$

OM%: Organic Matter

m_1 : Weight of the capsule and sample before calcination

m_2 : Weight of the capsule and sample after calcination

TE: Test portion

The ash content was calculated as follows (formula 3):

The ash content was calculated as follows (formula 3):

$$Ash\ \% = 100 - OM\% \quad (3)$$

Heavy Metal Analysis: Inductively Coupled Plasma Atomic Emission Spectrometry (ICP-AES)

The analysis of the heavy metals in *A. graveolens* seeds was conducted using the technique of Inductively Coupled Plasma Atomic Emission Spectrometry according to the standardized mineralization protocol [71].

This method involved first preparing the sample for analysis in liquid form by mixing 0.1 g of plant powder with 3 mL of aqua regia prepared from 1 mL of nitric acid HNO_3 (99%) and 2 mL of hydrochloric acid HCl (37%), all placed in a reflux setup at 200 °C for two hours to ensure the complete dissolution of residual metal particles. Following the process of chilling and decantation, the liquid remaining above the sediment was gathered. It was then passed through a filter with a pore size of 0.45 μm and brought to a volume of 15 mL by adding distilled water. The concentrations of the heavy metals including arsenic (As), cadmium (Cd), chromium (Cr), iron (Fe), lead (Pb), antimony (Sb), and titanium (Ti) were quantified using an Inductively Coupled Plasma Atomic Emission Spectrometer (Ultima 2 Jobin Yvon) at the laboratory of UATRS (Technical

Support Unit for Scientific Research) at CNRST in Rabat.

Phytochemical Screening

This is a qualitative analysis that allows for the identification of primary and secondary metabolites present in *A. graveolens* seeds. These tests were based on the visual observation of color changes, and formation of precipitates and complexes, while other tests included the examination of the samples under UV light. The detection of chemical compound groups was carried out according to protocols described in previous studies [72–77].

Extraction and Quality Control of Essential Oils

Extraction and Determination of Essential Oil Yields

The extraction of essential oils from *A. graveolens* seed was carried out by hydrodistillation. A total of 100 g of dried dill seeds were immersed in a 2 L flask containing 1 L of water, topped with a Clevenger apparatus and a ball-type condenser. The mixture was brought to a boil for 3 h. The oils obtained were subsequently dehydrated using anhydrous sodium sulfate (Na_2SO_4) and kept in a sealed brown glass container at a temperature of 4 °C until they were ready for use. The extraction yield of the essential oil was quantified as the volume of essential oil obtained per unit mass of plant material (v/m), using formula (4) [78].

$$\% \text{Yield} = \frac{V}{m_0 - (m_0 \times \% \text{MC})}$$

MC(%): Percentage of moisture in the plant material (moisture content). m_0 : Mass of distilled plant material

V: Volume of collected essential oil (in mL).

Analysis and Identification of the Chemical Composition of Essential Oils

The chromatographic analysis of essential oils was performed on a gas chromatograph of the Thermo Electron type (Trace GC Ultra) coupled with a mass spectrometer of the Thermo Electron Trace MS system (Thermo Electron: Trace GC Ultra; Polaris Q MS), with fragmentation carried out by electron impact at a 70 eV intensity. The chromatograph is equipped with a DB-5 type column (5% phenyl-methylsiloxane) (30 m × 0.25 mm × 0.25 μm film thickness) and a flame ionization detector (FID) powered by an H_2 /Air gas mixture. The column temperature was programmed to increase by 4 °C/min from 50 to 200 °C for 5 min. The injection mode was split (leak ratio: 1/70, flow rate mL/min), and the carrier gas used was nitrogen at a flow rate of 1 mL/min.

The identification of the chemical composition of essential oils was performed by comparing their calculated Kovats indices (IK) with those of Adams and known reference products in the literature [79–81]. This was accomplished by conducting a comparison of the retention indices and mass spectra with those found in the mass spectral libraries of the National Institute of Standards and Technologies (NIST). Additionally, the experimental retention indices were compared with those available in the NIST online data collection at <https://webbook.nist.gov/chemistry/name-ser/> (accessed on 10 April 2024). The proportions of each component were automatically determined using the total ion count observed by the GC-MS and represented as a percentage composition.

Extraction of Phenolic Compounds

To begin with, in order to isolate the phenolic compounds, two extraction methods were employed: decoction and solid–liquid extraction using the Soxhlet apparatus. The decoction procedure consisted of adding 30 g of the sample to 600 mL of distilled water and heating and bringing the mixture to a boil for one hour at 80 °C. After a five-minute decantation, the mixture was filtered under reduced pressure, and the decocted extract was recovered. This extract was then dried in an oven at 70 °C and subsequently stored in a glass vial.

As for the solid–liquid extraction, it was carried out using the Soxhlet apparatus on two additional samples weighing 30 g each. Two extraction solvents were used: pure water and a 10/1 v/v standard deviation of 70/30. The extracts were concentrated using a rotary evaporator after several extraction cycles. These extracts were then identified, as indicated in Table 15.

Table 15. Coding of *A. graveolens* extracts.

Extraction Methods	Solvents	Coding
Decoction	Water	E (0)
	Ethanol/water(70/30;v/v)	E (1)
Soxhlet	Water	E (2)

Quantification of Phenolic Compounds

The total phenolic content of the different extracts was determined using the Folin–Ciocalteu method described by Singleton and Rossi [82]. This method is based on the reduction in the basic medium of the mixture of phosphotungstic acid $H_3P(W_3O_{10})_4$ and phosphomolybdic acid $H_3PMO_{12}O_4$ by the oxidizable groups of phenolic compounds present in various *A. graveolens* extracts. The chemical compounds tungsten oxide (W_8O_{23}) and molybdenum oxide (Mo_8O_3), which have a blue tint, were examined using colorimetry and optical density measurement. The absorbance measurement was acquired using a UV mini-1240 spectrophotometer configured at a wavelength of 760 nm and then compared to a blank sample, which consisted of a reaction mixture without the extract. A calibration curve was created in parallel, using the same working conditions, with a concentration range of 0.05 to 50 $\mu\text{g/mL}$ of gallic acid as a positive control. The total phenolic content was determined by applying the calibration curve equation ($Y=0.095X+0.003$; $R^2=0.998$), and the results were expressed in milligrams of gallic acid equivalent per gram of extract (mg GAE/g). The experiment was replicated thrice.

Quantification of Flavonoids

The method by Djeridane and colleagues was used to determine the flavonoid content of our samples using aluminum trichloride as a reagent [83]. The technique is based on the oxidation of flavonoids by this reagent, leading to the formation of a stable yellowish flavonoid–aluminum complex, detectable in the visible range at 433 nm. The flavonoid content in our samples was determined from a calibration range established with increasing concentrations of quercetin ranging from 5 to 30 $\mu\text{g/mL}$, with the linear regression equation of $Y=0.073X-0.081$ and a determination coefficient R^2 equal to 0.995. The flavonoid content was expressed in milligrams of quercetin equivalent per gram of extract (mg EQ/g). Each test was repeated three times.

Quantification of Condensed Tannins

The vanillin method was employed to evaluate the concentrations of condensed tannins [84]. During this process, a solution containing vanillin dissolved in

methanol at a concentration of 4% w/v was combined with 20 μL portions of the extracts or a solution of (+)-catechin at a concentration of 2 mg/mL. Subsequently, the mixtures were manually agitated. Subsequently, each concentration was transferred to a test tube containing 1.5 mL of hydrochloric acid. The reaction mixture was allowed to stand at ambient temperature for a duration of 20 min. The measurement of absorbance was conducted at a wavelength of 499 nm using a UV–visible spectrophotometer, with a reference to a blank sample. The content of condensed tannins in the samples was calculated from the catechin calibration curve used as a standard ($Y=0.7421X+0.0318$; $R^2=0.998$). The tannin content was expressed in milligrams of catechin equivalent per gram of extract (mg EC/g).

HPLC/UV-ESI-MS Analysis of *A. graveolens* Seed Extracts

The phenolic components of *A. graveolens* in the decoction were analyzed using High-performance liquid chromatography combined with a QEx active Plus mass spectrometer and electrospray ionization as the molecular ionization method (HPLC/UV-ESI-MS). The analysis was performed on an UltiMate 3000 HPLC system (Thermo Fisher Scientific, Sunnyvale, CA, USA) with an autosampler maintained at 5°C. The HPLC system

employed a reverse-phase C18 column with a column temperature of 40°C (LichroCART, Lichrospher, Merck, Darmstadt, Germany, 250 × 4 mm, ID 5 µm). The mobile phase was composed of solvent A, which was a mixture of 0.1% formic acid in water (v/v), and solvent B, which was a mixture of 0.1% formic acid in acetonitrile (v/v). The gases were eliminated from the mobile phase using the process of sonication. The description of the gradient's composition may be found in Supplementary Table S1. The rate of flow was 1 milliliter per minute, and the amount injected was 20 µL. After negative electrospray ionization, broadband collision-induced dissociation (bbCID) detection was carried out using a Maxis Impact HD instrument (Bruker Daltonik, Bremen, Germany). The UV detection in the range of 190 to 600 nm and acquisition of three wavelengths from 280 to 320 to 360 nm were performed using a diode array detector L-2455 (Merck-Hitachi, Darmstadt, Germany). The parameters used were a capillary voltage of 3000 V, drying gas temperature of 200°C, dry gas flow rate of 8 L/min, nebulizer gas pressure of 2 bars, and offset voltage of 500 V. Nitrogen was used as both the nebulizer and desolvation gas. The *m/z* range of the MS data was from 100 to 1500.

The process of gathering and examining data was $AA\% =$

$AA\%$: Percentage of antioxidant activity.

A_{control} : Absorbance of the solution containing only the DPPH• radical solution. A_{sample} : Absorbance of the test sample solution in the presence of DPPH•.

The 50% inhibitory concentration of the DPPH• free radicals (IC_{50}) for BHT or our extracts was determined from a graph of antioxidant activity variation with concentration.

Ferric Reducing Antioxidant Power (FRAP) Method

Using the method described by Oyaizu [86], the ability of the phenolic extracts from *A. graveolens* to convert ferric iron (Fe^{3+}) in the potassium ferricyanide complex to ferrous iron (Fe^{2+}) was evaluated. One millilitre of the plant extract under investigation was combined with 2.5 millilitres of a phosphate buffer solution (0.2M, pH 6.6) and 2.5 millilitres of a potassium ferricyanide solution ($K_3Fe(CN)_6$ at a concentration of 1%). The final combination was incubated for 20 minutes at 50°C in a water bath of varying temperatures. To stop the reaction's progression, 2.5 mL of a solution containing 10% trichloroacetic acid was then added. For ten minutes, the solution was centrifuged at a speed of three thousand revolutions per minute. Finally, 0.5 mL of a solution containing 0.1% $FeCl_3$ dissolved in water, 2.5 mL of pure water, and 2.5 mL of the liquid that remained after centrifugation from each concentration were mixed together. A UV-Vis spectrophotometer was used to measure the absorbance of the reaction medium

conducted using Thermo Scientific's Chromeleon 7.2 chromatography data system (CDS). The eluted chemicals were analyzed by studying the mass spectra of the isolated molecules.

Antioxidant Activity

Radical Scavenging Activity by DPPH• Test

The antioxidant activity of the essential oils (EO) and extracts of *A. graveolens* was assessed using the 2,2-diphenyl-1-picrylhydrazyl (DPPH) radical, following the procedure outlined by [85]. A total of 200 µL of *A. graveolens* extract or EO was applied to test tubes containing 100% ethanol. Afterward, 2.8 mL of a solution of DPPH• in ethanol (24 µg/mL, w/v) was added to the mixture and allowed to incubate for 30 min in the absence of light. The measurement of absorbance was conducted at a wavelength of 515 nm using a UV-Vis spectrophotometer. The experiments were replicated thrice. The reference standard utilized was butylated hydroxytoluene (BHT) at varying concentrations. The results were quantified as a percentage of DPPH• decrease, denoted as AA% (formula 5):

$A_{\text{control}} - A_{\text{sample}}$

A_{control}

× 100

(5)

at a wavelength of 700 nm. The same procedure was used to create a blank sample, except

For calibration purposes, the aqueous extract was substituted with distilled water. A solution of a common antioxidant, BHA (Butylated Hydroxyanisole), served as the positive control, and its absorbance was assessed in the same way as the samples. Every test was conducted three times. The concentration that corresponds to an absorbance of 0.5 (EC_{50}) was determined by graphing the change in reducing power as a function of BHT content of our extracts. Total Capacity of Antioxidants

To evaluate the overall antioxidant ability of *A. graveolens* extracts, the phosphomolybdenum assay, as reported by Khiya et al. [87], was used. This test is based on the fact that when extracts are present, molybdenum $Mo^{6+}(VI)$ is reduced to molybdenum $Mo^{5+}(V)$, forming a green complex called phosphate/ $Mo^{5+}(V)$ at an acidic pH with a maximum absorbance at 695 nm.

Three millilitres of the reactive solution—0.6 M sulphuric acid, 28 mM sodium phosphate, and 4 mM ammonium molybdate—were added to a volume of extract in a test tube. After shaking and 90 minutes at 95 °C in an incubator, the tubes were allowed to return to room temperature. The absorbance of the solutions was

measured at 695 nm after cooling. The standard utilised was ascorbic acid. The findings were reported as mg AAE/g, or milligrammes of ascorbic acid equivalents per gramme of extract.

Antimicrobial Activity

The lowest concentration of an essential oil extract that may totally stop a microorganism's development is known as the Minimum Inhibitory Concentration, or MIC. Utilising the microdilution technique, the MIC was determined [88]. Initially, a stock solution of essential oil made in 10% DMSO was treated to a series of dilutions to acquire concentrations for the essential oil ranging from 5 to 0.93×10^{-2} mg/mL. Regarding the extracts, a stock solution was made previously and diluted to reach the required concentrations, which were stated in $\mu\text{g/mL}$. A final volume of 100 μL was used for each concentration of essential oil and extracts, which were diluted in a Mueller–Hinton broth for bacteria and a Sabouraud broth for fungi.

The different concentrations of the dilution series were then supplemented with 100 μL of the microbial inoculum, which had a final concentration of 106CFU/mL for bacteria and 104CFU/mL for fungus. 10 μL of resazurin was added to each well as a method of measuring bacterial proliferation after a 24-hour incubation period at 37 °C. Following a second incubation time at 37°C, a change in colour from violet to ink showed the existence of microbial growth. The lowest concentration of a chemical that effectively prevents the observed colour shift of resazurin is known as the minimum inhibitory concentration, or MIC. Each series' growth control and sterility control were assigned to the eleventh and twelfth wells, respectively. For the oil and extracts, this method was repeated twice.

10 μL was extracted from each well that showed no signs of growth and inoculated on Mueller–Hinton agar (MH) for bacteria or Sabouraud agar for fungi in order to calculate the Minimum Bactericidal Concentration (MBC) or Minimum Fungicidal Concentration (MFC). The plates were incubated at 37 °C for 24 hours. As the lowest concentration of the samples examined, the MBC and MFC produced a 99.99% decrease in CFU/mL in comparison to the control. To evaluate the antibacterial power, the ratio of MBC/MIC or MFC/MIC was computed. The essential oil had a bactericidal or fungicidal effect if the ratio was less than 4, and a bacteriostatic or fungistatic effect if the ratio was larger than 4. PASS, ADMET, Pro-Tox, and Estimation of the

Effectiveness of Potentially Active Substances Derived from *A. graveolens* Seed Essential Oil and Aqueous Extract

The primary components of the aqueous extract and essential oil (EO) extracted from the seeds of *A. graveolens* that were analysed were chosen for PASS prediction tests and ADMET (absorption, distribution, metabolism, excretion, and toxicity) testing. Using ChemBioDraw (PerkinElmer Informatics, Waltham, MA, USA, v13.0) [56], the SMILES format of these chemicals was selected. The PASS-Way2DrugOnlinePredictionTool [57], together with the online tools SwissADME and pkCSM for ADMET prediction [58], were then used to run simulations. The PASS acronym was used to identify the likely inactivity (Pi) and possible activity (Pa) of "drug-like" compounds [89].

To assess toxicity levels and collect pertinent information on a number of toxicological parameters, such as LD50 and the toxicity class, ProTox II, a helpful tool designed especially for this purpose, was used [90]. To evaluate the selected ligands, the ADMET software—which includes SwissADME, pkCSM, and ProToxII—was used. Their physicochemical characteristics, lipophilicity, water solubility, pharmacokinetics, drug-likeness, medicinal chemistry, and toxicological aspects might all be predicted thanks to this. Reliable observations on the potential therapeutic applications and adverse effects associated with the main chemical constituents present in the EO and aqueous extract of *A. graveolens* seeds under study were made feasible by the use of these techniques and analytical tools.

Docking of Molecular Structures

The Protein Data Bank RCSB, which may be accessed at the URL <https://www.rcsb.org/>, provided the three-dimensional structures of the protein targets, as shown in Table 16. (retrieved April 10, 2024). UCSF Chimera was used to visualise the protein structure. The Autodock Tools (version 1.5.6, The Scripps Research Institute, La Jolla, CA, USA) were used to generate the protein structures as appropriate docking targets. The protein structures were preprocessed before analysis, which included removing co-crystallized ligands, water molecules, heteroatoms (hetatm), and undesired protein chains. Following the addition of polar hydrogen atoms and Gasteiger charges, the structures were transformed into pdbqt format for further examination.

Table 16. Protein targets and molecular docking parameters.

Protein	PDB ID	GridBoxCenter Coordinates	GridBoxSize
---------	--------	---------------------------	-------------

Isoleucyl-tRNA synthetase	1JZQ	center_x=-27.803	size_x= 34
		center_y=6.619	size_y=22
		center_z= -28.722	size_z= 21
DNA gyrase	1KZN	center_x=18.325	size_x= 23
		center_y=30.783	size_y=38
		center_z= 36.762	size_z= 38
Catalase compound II	2CAG	center_x=60.017	size_x= 28
		center_y=14.760	size_y=22
		center_z= 15.935	size_z= 34
Dihydropterotate synthase	2VEG	center_x=31.404	size_x= 24
		center_y=48.530	size_y=24
		center_z= 0.204	size_z= 23
D-Alanine ligase	2ZDQ	center_x=47.378	size_x= 21
		center_y=12.782	size_y=26
		center_z= 5.730	size_z= 32
Dihydrofolate reductase	3SRW	center_x=-4.701	size_x= 20
		center_y=-31.536	size_y=26

Protein Name	PDB ID	Simulation Details
Penicillin-binding protein 1a (PBP1a)	3UDI	Simulation details for PBP1a
Crystal structure of StaphParE (24 kDa)	4URN	Simulation details for StaphParE
NADPH oxidase	2CDU	Simulation details for NADPH oxidase
Cytochrome P450 2C9	1OG5	Simulation details for Cytochrome P450 2C9
Xanthine dehydrogenase/oxidase	3NRZ	Simulation details for Xanthine dehydrogenase/oxidase

The sixteen compounds' three-dimensional structures were obtained from PubChem, represented using their corresponding structures, and then structural energy minimisation was used. Following that, the ligands' SDF files were transformed into pdbqt formats using the Prescription Virtual Screening Python script (AutoDockVina1.2.0).

The scoring function of AutoDockVina was used in the compound docking process. A gridbox was superimposed on the protein structure after the selection of the protein and ligand molecules for docking in the Vinacontrol. Before starting the AutoDockVina software for the docking process, the gridbox size might be changed depending on the chosen active site residues. The gridbox, whose size and location were determined by coordinates exactly aligned with the active binding site, restricted the search space (Table 16). PyMOL was used to analyse the ligand-protein binding characteristics after the results for docked molecules were recorded and represented as free binding energy values.

We next moved on to redocking, which is a dependable technique for confirming the molecular docking procedure. Using this technique, the crystallised ligand is separated from the protein, and then a fresh docking analysis is conducted in the same region as the original ligand. By closely examining the RMSD parameter value using specialised software like PyMOL 2.5.0, we can determine whether the docked ligand effectively overlaps with the crystallised ligand. In conclusion, redocking provides rigorous validation of the molecular docking process by confirming the consistency of the results obtained. Simulation of Molecular Dynamics The stability of the protein-ligand combination was assessed using the GROMACS2019.3 program in order to conduct molecular dynamics simulations [91]. The all-atom CHARMM36 force field was applied to the protein, and the CGenFF service was used to create the

ligand topologies. After the fall complexes were centered in a regular cubic box containing TIP3P water molecules, the systems were made neutral by adding ions to balance the total charges. Using the steepest-descent technique, a force threshold (F_{max}) of 1000 kJ/mol/nm was chosen in order to get the least energy and highest force. For molecular dynamic simulation studies, the ensembles were kept at constant (number of atoms, volume, and temperature) and constant number of atoms, size, and pressure, and temperature). Every molecule was then subjected to 10 molecular dynamics simulation through gas phase protein behaviour was obtained by analysing output trajectory. Analytical Statistical The standard deviation is a measure of variability, where the average is a representation of the results. Tukey's post-test and a one-way ANOVA test were used to assess the data using GraphPad Prism 8 software (version 8.0.2, San Diego, CA, USA). It was determined

that P-values below 0.05 were significant. The Pearson correlation coefficient was used to evaluate the link between the phenolic components and antioxidant activity content. A statistically significant difference was defined as one where the P-value was less than 0.05.

4. Conclusions

The quantity of phytochemicals in *Anethum graveolens* seeds was highlighted in this research. GC-MS analysis of the essential oil revealed that the most abundant component was (E)-anethole, which was 38.13%, followed by estragole, which was 29.32%, fenchone, which was 17.21%, and α -pinene, which was 7.37%. Additionally, the seeds included secondary metabolites such as mucilage, sterols, triterpenes, flavonoids, and tannins.

Significant levels of polyphenols, flavonoids, and condensed tannins were found in this quantitative investigation. 38 important chemicals, including umbelliferone (12.35%), hydroxyflavone (11.23%), rosmanol (8.95%), biotin (8.36%), emmotin H (4.91%), and coumarin (4.21%), were detected and identified by the application of HPLC/UV-ESI-MS analysis.

The DPPH', FRAP, and CAT assays demonstrated the essential oils and extracts' strong antioxidant activity. They were able to bind metal ions and efficiently neutralise free radicals. The antimicrobial tests showed that the essential oil was more effective against most of the examined microorganisms than the aqueous, ethanolic, and decoction extracts. The synergistic effects of its main ingredients are responsible for this increased efficacy.

Significant relationships and long-lasting stability between certain bioactive compounds and a variety of target proteins were confirmed by the docking and molecular dynamics simulations. The results show that *A. graveolens* has a considerable

therapeutic potential for a variety of human illnesses and may be used as a natural food preservative. Additional Resources: You can download the supporting documentation at <https://www.mdpi.com/article/10.3390/ph17070862/s1>. Figure S1. GC-MS chromatogram of the essential oil from *A. graveolens*; Figure S2. Structures of the primary compounds identified in *A. graveolens*EO; Figure S3. HPLC chromatogram of compounds from the decocted extract of *A. graveolens*; Figure S4. Structure of the majority of compounds identified in extract E(0) of *A. graveolens*; Table S1. Gradient mobile phase elution.

References

- Mathers, C.; Organization, W.H. *The Global Burden of Disease: 2004 Update*; World Health Organization: Geneva, Switzerland, 2008; ISBN 978-92-4-156371-0.
- Zhang, X.-J.; Diao, M.; Zhang, Y.-F. A Review of the Occurrence, Metabolites and Health Risks of Butylated Hydroxyanisole (BHA). *J. Sci. Food Agric.* **2023**, *103*, 6150–6166. <https://doi.org/10.1002/jsfa.12676>.
- Ito, N.; Hirose, M.; Fukushima, S.; Tsuda, H.; Shirai, T.; Tatematsu, M. Studies on Antioxidants: Their Carcinogenic and Modifying Effect on Chemical Carcinogenesis. *Food Chem. Toxicol.* **1986**, *24*, 1071–1082. [https://doi.org/10.1016/0278-6915\(86\)90291-7](https://doi.org/10.1016/0278-6915(86)90291-7).
- Lopez-Romero, J.C.; González-Ríos, H.; Borges, A.; Simões, M. Antibacterial Effects and Mode of Action of Selected Essential Oils Components against *Escherichia Coli* and *Staphylococcus Aureus*. *Evid. Based Complement. Altern. Med.* **2015**, *2015*. <https://doi.org/10.1155/2015/795435>.
- Paven, C.S.J.; Radu, D.; Alexa, E.; Pintilie, S.; Rivis, A. *Anethum Graveolens*—An Important Source of Antioxidant Compounds for Food Industry. *Adv. Biotechnol.* **2018**, *18*, 11–18. <https://doi.org/10.5593/sgem2018/6.2/S25.002>.
- Jana, S.; Shekhawat, G. *Anethum Graveolens*: An Indian Traditional Medicinal Herb and Spice. *Pharmacogn. Rev.* **2010**, *4*, 179–184. <https://doi.org/10.4103/0973-7847.70915>.
- Brinsi, C.; Selmi, H.; Jedidi, S.; Sebai, H. Enquête Ethno-Pharmacologique Sur l' Usage Traditionnel de l'Aneth (*Anethum Graveolens* L.) Dans Le Nord-Ouest de La Tunisie. *Rev. Marocaine Des Sci. Agron. Et Vétérinaires* **2022**, *10*, 282–286.
- Jirovetz, L.; Buchbauer, G.; Stoyanova, A.S.; Georgiev, E.V.; Damianova, S.T.; Composition, Quality Control, and Antimicrobial Activity of the Essential Oil of Long-Time Stored Dill (*Anethum Graveolens*, L.) Seeds from Bulgaria. *J. Agric. Food Chem.* **2003**, *51*, 3854–3857. <https://doi.org/10.1021/jf030004y>.
- Kaur, N.; Chahal, K.K.; Kumar, A.; Singh, R.; Bhardwaj, U. Antioxidant Activity of *Anethum Graveolens*, L. Essential Oil Constituents and Their Chemical Analogues. *J. Food Biochem.* **2019**, *43*, e12782. <https://doi.org/10.1111/jfbc.12782>.
- Nam, H.H.; Nan, L.; Choo, B.K. Anti-Inflammation and Protective Effects of *Anethum Graveolens* L. (Dill Seeds) on Esophageal Mucosa Damages in Reflux Esophagitis-Induced Rats. *Foods* **2021**, *10*. <https://doi.org/10.3390/foods10102500>.
- Goodarzi, M.T.; Khodadadi, I.; Tavilani, H.; Abbasi Oshaghi, E. The Role of *Anethum Graveolens*, L. (Dill) in the Management of Diabetes. *J. Trop. Med.* **2016**, *2016*. <https://doi.org/10.1155/2016/1098916>.
- Ozliman, S.; Yaldiz, G.; Camlica, M.; Ozsoy, N. Chemical Components of Essential Oils and Biological Activities of the Aqueous Extract of *Anethum Graveolens*, L. Grown under Inorganic and Organic Conditions. *Chem. Biol. Technol. Agric.* **2021**, *8*, 1–16. <https://doi.org/10.1186/s40538-021-00224-9>.
- Mahran, G.H.; Kadry, H.A.; Isaac, Z.G.; Thabet, C.K.; Al-Azizi, M.M.; El-Olemy, M.M. Investigation of Diuretic Drug Plants. 1. Phytochemical Screening and Pharmacological Evaluation of *Anethum Graveolens*, L., *Apium Graveolens*, L., *Daucus Carota*, L. and *Eruca Sativa* Mill. *Phytother. Res.* **1991**, *5*, 169–172. <https://doi.org/10.1002/ptr.2650050406>.
- Najafzadeh, R.; Ghasemzadeh, S.; Mirfakhraie, S. Effect of Essential Oils from *Nepeta Crispa*, *Anethum Graveolens* and *Satureja Hortensis* Against the Stored-Product Insect “*Ephestia kuehniella* (Zeller).” *J. Med. Plants By-Prod.* **2019**, *2*, 163–169.
- Rabeh, N.M.; Aboraya, A.O. Hepatoprotective Effect of Dill (*Anethum Graveolens*, L.) and Fennel (*Foeniculum Vulgare*) Oil on Hepatotoxic Rats. *Pak. J. Nutr.* **2014**, *13*, 303–309. <https://doi.org/10.3923/pjn.2014.303.309>.
- Al-Oqail, M.M.; Farshori, N.N. Antioxidant and Anticancer Efficacies of *Anethum Graveolens* against Human Breast Carcinoma Cells through Oxidative Stress and Caspase Dependency. *BioMed Res. Int.* **2021**, *2021*. <https://doi.org/10.1155/2021/5535570>.
- El-Sayed, K.K.; El-Sheikh, E.-S.A.; Sherif, R.M.; Gouhar, K.A. Chemical Composition and Bio-Efficacy of Essential Oils Isolated from Seeds of *Anethum Graveolens*, L., Leaves of *Thymus Vulgaris*, L., and Nuts of *Myristica Fragrans* Houtt. Against *Callosobruchus Maculatus* (Fab.) (Coleoptera: Bruchidae). *J. Essent. Oil Bear. Plants* **2021**, *24*, 1402–1414. <https://doi.org/10.1080/0972060X.2021.2016498>.
- Farmanpour Kalalagh, K.; Mohebodini, M.; Fattahi,

- R.; Beyraghdar Kashkooli, A.; Davarpanah Dizaj, S.; Salehifar, F.; Mokhtari, A.M. Drying Temperatures Affect the Qualitative–Quantitative Variation of Aromatic Profiling in *Anethum Graveolens*, L. Ecotypes as an Industrial–Medicinal–Vegetable Plant. *Front. Plant Sci.* **2023**, *14*. <https://doi.org/10.3389/fpls.2023.1137840>.
19. Mehdizadeh, T.; Mojaddar Langroodi, A.; Shakouri, R.; Khorshidi, S.; Physicochemical, Microbiological, and Sensory Characteristics of Probiotic Yogurt Enhanced with *Anethum Graveolens* Essential Oil. *J. Food Saf.* **2019**, *39*, e12683. <https://doi.org/10.1111/jfs.12683>.
 20. Znini, M.; Ansari, A.; Costa, J.; Senhaji, O.; Paolini, J.; Majidi, L.; Experimental, Quantum Chemical and Molecular Dynamic Simulations Studies on the Corrosion Inhibition of C38 Steel in 1M HCl by *Anethum Graveolens* Essential Oil. *Anal. Bioanal. Electrochem* **2019**, *11*, 1426–1451.
 21. Li, H.; Zhou, W.; Hu, Y.; Mo, H.; Wang, J.; Hu, L. GC-MS Analysis of Essential Oil from *Anethum Graveolens* L (Dill) Seeds Extracted by Supercritical Carbon Dioxide. *Trop. J. Pharm. Res.* **2019**, *18*, 1291–1296. <https://doi.org/10.4314/tjpr.v18i6.21>.
 22. Snuossi, M.; Trabelsi, N.; Ben Taleb, S.; Dehmeni, A.; Flamini, G.; De Feo, V. Laurus Nobilis, Zingiber Officinale and *Anethum Graveolens* Essential Oils: Composition, Antioxidant and Antibacterial Activities against Bacteria Isolated from Fish and Shellfish. *Molecules* **2016**, *21*, 1414. <https://doi.org/10.3390/molecules21101414>.
 23. Noumi, E.; Ahmad, I.; Adnan, M.; Merghni, A.; Patel, H.; Haddaji, N.; Bouali, N.; Alabbosh, K.F.; Ghannay, S.; Aouadi, K.; et al. GC/MS Profiling, Antibacterial, Anti-Quorum Sensing, and Antibiofilm Properties of *Anethum Graveolens*, L. Essential Oil: Molecular Docking Study and In-Silico ADME Profiling. *Plants* **2023**, *12*, 1997. <https://doi.org/10.3390/plants12101997>.
 24. Kostić, I.; Lazarević, J.; Šešlija Jovanović, D.; Kostić, M.; Marković, T.; Milanović, S. Potential of Essential Oils from Anise, Dill and Fennel Seeds for the Gypsy Moth Control. *Plants* **2021**, *10*, 2194. <https://doi.org/10.3390/plants10102194>.
 25. Aati, H.Y.; Perveen, S.; Aati, S.; Orfali, R.; Alqahtani, J.H.; Al-Taweel, A.M.; Wanner, J.; Aati, A.Y. Headspace Solid-Phase Microextraction Method for Extracting Volatile Constituents from the Different Parts of Saudi *Anethum Graveolens*, L. and Their Antimicrobial Activity. *Heliyon* **2022**, *8*. <https://doi.org/10.1016/j.heliyon.2022.e09051>.
 26. Anvar, N.; Nateghi, L.; Shariatifar, N.; Mousavi, S. A. The Effect of Essential Oil of *Anethum Graveolens*, L. Seed and Gallic Acid (Free and Nano Forms) on Microbial, Chemical and Sensory Characteristics in Minced Meat during Storage at 4°C. *Food Chem. X* **2023**, *19*, 100842. <https://doi.org/10.1016/j.fochx.2023.100842>.
 27. El Mansouri, L.; Bousta, D.; Balouiri, M.; Ouedrhiri, W.; Elyoubi-El Hamsas, A. Antioxidant Activity of Aqueous Seed Extract of *Anethum Graveolens*, L. *Int. J. Pharm. Sci. Res.* **2016**, *7*, 1219–1223. [https://doi.org/10.13040/IJPSR.0975-8232.7\(3\).1219-23](https://doi.org/10.13040/IJPSR.0975-8232.7(3).1219-23).
 28. Bota, S.R.; Stanasel, O.D.; Blidar, C.F.; Serban, G.P. Phenolic Constituents of *Anethum Graveolens* Seed Extracts: Chemical Profile and Antioxidant Effect Studies. *J. Pharm. Res. Int.* **2021**, *33*, 168–179. <https://doi.org/10.9734/jpri/2021/v33i54b33777>.
 29. Mashraqi, A. Induction Role of Chitosan Nanoparticles to *Anethum Graveolens* Extract against Food-Borne Bacteria, Oxidant, and Diabetic Activities in Vitro. *Front. Microbiol.* **2023**, *14*, 1–12. <https://doi.org/10.3389/fmicb.2023.1209524>.
 30. Erdogan Orhan, I.; Senol, F.S.; Ozturk, N.; Celik, S.A.; Pulur, A.; Kan, Y. Phytochemical Contents and Enzyme Inhibitory and Antioxidant Properties of *Anethum Graveolens*, L. (Dill) Samples Cultivated under Organic and Conventional Agricultural Conditions. *Food Chem. Toxicol.* **2013**, *59*, 96–103. <https://doi.org/10.1016/j.fct.2013.05.053>.
 31. Meena, S.S.; Lal, G.; Dubey, P.N.; Meena, M.D.; Ravi, Y. Medicinal and Therapeutic Uses of Dill (*Anethum Graveolens* L.)—A Review. *Int. J. Seed Spices* **2019**, *9*, 14–20.
 32. Sharifi-Rad, J.; Cruz-Martins, N.; López-Jornet, P.; Lopez, E.P.F.; Harun, N.; Yeskalyeva, B.; Beyatli, A.; Sytar, O.; Shaheen, S.; Sharopov, F.; et al. Natural Coumarins: Exploring the Pharmacological Complexity and Underlying Molecular Mechanisms. *Oxidative Med. Cell. Longev.* **2021**, *2021*. <https://doi.org/10.1155/2021/6492346>.
 33. Mazimba, O. Umbelliferone: Sources, Chemistry and Bioactivities Review. *Bull. Fac. Pharm. Cairo Univ.* **2017**, *55*, 223–232. <https://doi.org/10.1016/j.bfopcu.2017.05.001>.
 34. Chen, S.; Wang, X.; Cheng, Y.; Gao, H.; Chen, X. A Review of Classification, Biosynthesis, Biological Activities and Potential Applications of Flavonoids. *Molecules* **2023**, *28*, 1–27. <https://doi.org/10.3390/molecules28134982>.
 35. Thomas, S.D.; Jha, N.K.; Jha, S.K.; Sadek, B.; Ojha, S. Pharmacological and Molecular Insight on the Cardioprotective Role of Apigenin. *Nutrients* **2023**, *15*. <https://doi.org/10.3390/nu15020385>.
 36. Abid, R.; Ghazanfar, S.; Farid, A.; Sulaman, S.M.; Idrees, M.; Amen, R.A.; Muzammal, M.; Shahzad, M.K.; Mohamed, M.O.; Khaled, A.A.; et al. Pharmacological Properties

- of 4',5, 7-Trihydroxyflavone (Apigenin) and Its Impact on Cell Signaling Pathways. *Molecules* **2022**, *27*, 1–20. <https://doi.org/10.3390/molecules27134304>.
37. Maneesai, P.; Potue, P.; Khamseekeaw, J.; Sangartit, W.; Rattanakanokchai, S.; Poasakate, A.; Pakdeechote, P. Kaempferol Protects against Cardiovascular Abnormalities Induced by Nitric Oxide Deficiency in Rats by Suppressing the TNF- α Pathway. *Eur. J. Pharmacol.* **2023**, *960*, 176112. <https://doi.org/10.1016/j.ejphar.2023.176112>.
38. Deng, H.; Xu, Q.; Guo, H.Y.; Huang, X.; Chen, F.; Jin, L.; Quan, Z.S.; Shen, Q.K. Application of Cinnamic Acid in the Structural Modification of Natural Products: A Review. *Phytochemistry* **2023**, *206*, 113532.
39. Ruwizhi, N.; Aderibigbe, B.A. Cinnamic Acid Derivatives and Their Biological Efficacy. *Int. J. Mol. Sci.* **2020**, *21*, 1–36. <https://doi.org/10.3390/ijms21165712>.
40. Babaeenezhad, E.; Nouryazdan, N.; Nasri, M.; Ahmadvand, H.; Moradi Sarabi, M. Cinnamic Acid Ameliorate Gentamicin-Induced Liver Dysfunctions and Nephrotoxicity in Rats through Induction of Antioxidant Activities. *Heliyon* **2021**, *7*, e07465. <https://doi.org/10.1016/j.heliyon.2021.e07465>.
41. Koczurkiewicz-Adamczyk, P.; Kłaś, K.; Gunia-Krzyżak, A.; Piska, K.; Andrysiak, K.; Stępniewski, J.; Lasota, S.; Wójcik-Pszczola, K.; Dulak, J.; Madeja, Z.; et al. Cinnamic Acid Derivatives as Cardioprotective Agents against Oxidative and Structural Damage Induced by Doxorubicin. *Int. J. Mol. Sci.* **2021**, *22*. <https://doi.org/10.3390/ijms22126217>.
42. Osanloo, M.; Ghanbariasad, A.; Taghinezhad, A. Antioxidant and Anticancer Activities of Anethum Graveolens, L., Citrus Limon (L.) Osbeck and Zingiber Officinale Roscoe Essential Oils. *Tradit. Integr. Med.* **2021**, 333–347. <https://doi.org/10.18502/tim.v6i4.8266>.
43. Gladikostić, N.; Ikonić, B.; Teslić, N.; Zeković, Z.; Božović, D.; Putnik, P.; Bursać Kovačević, D.; Pavlič, B. Essential Oils from Apiaceae, Asteraceae, Cupressaceae and Lamiaceae Families Grown in Serbia: Comparative Chemical Profiling with In Vitro Antioxidant Activity. *Plants* **2023**, *12*, 745. <https://doi.org/10.3390/plants12040745>.
44. Stanojević, L.P.; Radulović, N.S.; Djokić, T.M.; Stančković, B.M.; Ilić, D.P.; Cakić, M.D.; Nikolić, V.D. The Yield, Composition and Hydrodistillation Kinetics of the Essential Oil of Dill Seeds (*Anethi Fructus*) Obtained by Different Hydrodistillation Techniques. *Ind. Crops Prod.* **2015**, *65*, 429–436. <https://doi.org/10.1016/j.indcrop.2014.10.067>.
45. Galicka, A.; Krętowski, R.; Nazaruk, J.; Cechowska-Pasko, M. Anethole Prevents Hydrogen Peroxide-Induced Apoptosis and Collagen Metabolism Alterations in Human Skin Fibroblasts. *Mol Cell Biochem* **2014**, *394*, 217–224. <https://doi.org/10.1007/s11010-014-2097-0>.
46. Donati, M.; Mondin, A.; Chen, Z.; Miranda, F.M.; do Nascimento Jr, B.B.; Schirato, G.; Pastore, P.; Frolidi, G. Radical Scavenging and Antimicrobial Activities of Croton Zehntneri, Pterodon Emarginatus and Schinopsis Brasiliensis Essential Oils and Their Major Constituents: Estragole, Trans-Anethole, β -Caryophyllene and Myrcene. *Nat. Prod. Res.* **2015**, *29*, 939–946. <https://doi.org/10.1080/14786419.2014.964709>.
47. Senatore, F.; Oliviero, F.; Scandolera, E.; Tagliatalata-Scafati, O.; Roscigno, G.; Zaccardelli, M.; DeFalco, E. Chemical Composition, Antimicrobial and Antioxidant Activities of Anethole-Rich Oil from Leaves of Selected Varieties of Fennel [*Foeniculum Vulgare* Mill. Ssp. *Vulgare* Var. *Azoricum* (Mill.) Thell]. *Fitoterapia* **2013**, *90*, 214–219. <https://doi.org/10.1016/j.fitote.2013.07.021>.
48. Luís, Â.; Sousa, S.; Wackerlig, J.; Dobusch, D.; Duarte, A.P.; Pereira, L.; Domingues, F. Star Anise (*Illicium Verum* Hook. f.) Essential Oil: Antioxidant Properties and Antibacterial Activity against *Acinetobacter Baumanni*. *Flavour Fragr. J.* **2019**, *34*, 260–270. <https://doi.org/10.1002/ffj.3498>.
49. Singh, S.; Das, S.; Singh, G.; Perotti, M.; Schuff, C.; Citalan, C. Comparative Studies of Chemical Composition, Antioxidant and Antimicrobial Potentials of Essential Oils and Oleoresins Obtained from Seeds and Leaves of Anethum Graveolens, L. *Toxicol. Open Access* **2017**, *3*, 2–9.
50. Coêlho, M.L.; Islam, M.T.; Layson da Silva Oliveira, G.; Oliveira Barros de Alencar, M.V.; Victor de Oliveira Santos, J.; Campinho dos Reis, A.; Oliveira Ferreira da Mata, A.M.; Correia Jardim Paz, M.F.; Docea, A.O.; Calina, D.; et al. Cytotoxic and Antioxidant Properties of Natural Bioactive Monoterpenes Nerol, Estragole, and 3,7-Dimethyl-1-Octanol. *Adv. Pharmacol. Pharm. Sci.* **2022**, *2022*, e8002766. <https://doi.org/10.1155/2022/8002766>.
51. El Omari, N.; Balahbib, A.; Bakrim, S.; Benali, T.; Ullah, R.; Alotaibi, A.; Naceiri Elmrbati, H.; Goh, B.H.; Ong, S.-K.; Ming, L.C.; et al. Fenchone and Camphor: Main Natural Compounds from Lavandula Stoechas, L., Expediting Multiple In Vitro Biological Activities. *Heliyon* **2023**, *9*, e21222. <https://doi.org/10.1016/j.heliyon.2023.e21222>.
52. Singh, A.; Raja, W. Assessment of Antioxidant Activity of Foeniculum Vulgare Seed Extract Using Fenton Reaction. *Res. J. Med. Plants Ayurveda* **2020**, *1*, 1–7.
53. Basavegowda, J.; Raveesha, K.A.R.; Amruthesh, K.

- .N.BioactivityandPhytochemicalStudiesofSeedExtractsofAnethumGraveolens Linn. *Let. Appl. NanoBioScience* **2022**, *11*, 3560–3572. <https://doi.org/10.33263/LIANBS112.35603572>
54. Kaur, G.J.; Arora, D.S. Antibacterial and Phytochemical Screening of Anethum Graveolens, Foeniculum Vulgare and Trachyspermum Ammi. *BMC Complement. Altern. Med.* **2009**, *9*, 1–10. <https://doi.org/10.1186/1472-6882-9-30>.
 55. Mota, A.S.; Rosário Martins, M.; Arantes, S.; Lopes, V.R.; Bettencourt, E.; Pombal, S.; Gomes, A.C.; Silva, L.A. Antimicrobial Activity and Chemical Composition of the Essential Oils of Portuguese Foeniculum Vulgare Fruits. *Nat. Prod. Commun.* **2015**, *10*, 673–676. <https://doi.org/10.1177/1934578x1501000437>.
 56. Li, Z.; Wan, H.; Shi, Y.; Ouyang, P. Personal Experience with Four Kinds of Chemical Structure Drawing Software: Review on ChemDraw, ChemWindow, ISIS/Draw, and ChemSketch. *J. Chem. Inf. Comput. Sci.* **2004**, *44*, 1886–1890. <https://doi.org/10.1021/ci049794h>.
 57. Filimonov, D.A.; Lagunin, A.A.; Glorizova, T.A.; Rudik, A.V.; Druzhilovskii, D.S.; Pogodin, P.V.; Poiroikov, V.V. Prediction of the Biological Activity Spectra of Organic Compounds Using the Pass Online Web Resource. *Chem Heterocycl Comp* **2014**, *50*, 444–457. <https://doi.org/10.1007/s10593-014-1496-1>.
 58. Daina, A.; Michielin, O.; Zoete, V. SwissADME: A Free Web Tool to Evaluate Pharmacokinetics, Drug-Likeness and Medicinal Chemistry Friendliness of Small Molecules. *Sci. Rep.* **2017**, *7*, 42717.
 59. Najaran, Z.T.; Hassanzadeh, M.K.; Nasery, M.; Emami, S.A. Dill (*Anethum Graveolens*, L.) Oils. In *Essential Oils in Food Preservation, Flavor and Safety*; Preedy, V.R., Ed.; Academic Press: San Diego, CA, USA, 2016; pp. 405–412. ISBN 978-0-12-416641-7.
 60. Madhuri, J.V. Bioactivity of *Anethum Graveolens*—An In Silico Approach. *New Vis. Biol. Sci.* **2022**, *13*, 85.
 61. Suriyarak, S.; Bayrasy, C.; Schmidt, H.; Villeneuve, P.; Weiss, J. Impact of Fatty Acid Chain Length of Rosmarinate Esters on Their Antimicrobial Activity against *Staphylococcus Carnosus* LTH1502 and *Escherichia Coli* K-12 LTH4263. *J Food Prot* **2013**, *76*, 1539–1548. <https://doi.org/10.4315/0362-028X.JFP-12-254>.
 62. Lin, L.; Dong, Y.; Zhao, H.; Wen, L.; Yang, B.; Zhao, M. Comparative Evaluation of Rosmarinic Acid, Methyl Rosmarinate and Pedalitin Isolated from *Rabdosia Serra* (MAXIM.) HARA as Inhibitors of Tyrosinase and α -Glucosidase. *Food Chem* **2011**, *129*, 884–889. <https://doi.org/10.1016/j.foodchem.2011.05.039>.
 63. Yuan, H.; Lu, W.; Wang, L.; Shan, L.; Li, H.; Huang, J.; Sun, Q.; Zhang, W. Synthesis of Derivatives of Methyl Rosmarinate and Their Inhibitory Activities against Matrix Metalloproteinase-1 (MMP-1). *Eur J Med Chem* **2013**, *62*, 148–157. <https://doi.org/10.1016/j.ejmech.2012.09.047>.
 64. Woo, E.-R.; Piao, M.S. Antioxidative Constituents from *Lycopus Lucidus*. *Arch Pharm Res* **2004**, *27*, 173–176. <https://doi.org/10.1007/BF02980102>.
 65. Koriem, K.M.M. Caftaric Acid: An Overview on Its Structure, Daily Consumption, Bioavailability and Pharmacological Effects. *Biointerface Res. Appl. Chem* **2020**, *10*, 5616–5623.
 66. Parveen, S.; Bhat, I.U.H.; Bhat, R. Kaempferol and Its Derivatives: Biological Activities and Therapeutic Potential. *Asian Pac. J. Trop. Biomed.* **2023**, *13*, 411. <https://doi.org/10.4103/2221-1691.387747>.
 67. Tambe, V.; Ditani, A.; Rajpoot, K.; Tekade, R.K. Chapter 4—Pharmacokinetics Aspects of Structural Modifications in Drug Design and Therapy. In *Biopharmaceutics and Pharmacokinetics Considerations*; Tekade, R.K., Ed.; Advances in Pharmaceutical Product Development and Research; Academic Press: Cambridge, MA, USA, 2021; Volume 1, pp. 83–108. ISBN 978-0-12-814425-1.
 68. Hirano, Y.; Okimoto, N.; Fujita, S.; Taiji, M. Molecular Dynamics Study of Conformational Changes of Tankyrase 2 Binding Subsites upon Ligand Binding. *ACS Omega* **2021**, *6*, 17609–17620. <https://doi.org/10.1021/acsomega.1c02159>.
 69. AFNOR NF V03-402. Épices et Aromates—Détermination de la Teneur en Eau—Méthode par Entraînement. Available online: <https://www.boutique.afnor.org/fr-fr/norme/nf-v03402/epices-et-aromates-determination-de-la-teneur-en-eau-methode-par-entrainement/fa032462/325> (accessed on 4 October 2021).
 70. Ph. Eur. 11.0.0125(04/2023), 2022 Animal Feeding Stuffs—Determination of Crude Ash. ISO: Geneva, Switzerland, 2022.
 71. Skujins, S. *Handbook for ICP-AES (Varian-Vista): A Short Guide to Vista Series ICP-AES Operation*; Varian Int. AG: Zug, Switzerland, 1998; p. 1.
 72. Dohou, N.; Yamni, K.; Tahrouch, S.; Idrissi Hassani, L.M.; Badoc, A.; Gmira, N. Screening Phytochimique d'une Endémique Ibéro-Marocaine, *Thymelaea Lythroides*. *Bull. De La Société De Pharm. De Bordx.* **2003**, *142*, 61–78.
 73. Mezzoug, N.; Elhadri, A.; Dallouh, A.; Amkiss, S.; Skali, N.S.; Abrini, J.; Zhiri, A.; Baudoux, D.; Diallo, B.; El Jaziri, M.; et al. Investigation of the Mutagenic and Antimutagenic Effects of *Origanum Compactum* Essential Oil and S

- omeofItsConstituents. *Mutat. Res. /Genet. Toxicol. Environ. Mutagen.* **2007**, 629, 100–110. <https://doi.org/10.1016/J.MRGENTOX.2007.01.011>.
74. Mogode,D.J.EtudePhytochimiqueetPharmacologiquedeCassiaNigricansVahl(Caesalpinaceae)UtiliséDansLeTraitement Des Dermatoses Au Tchad. Thèse de Doctorat, Université de N'Djaména, Abidjan, Tchad, 2005.
75. Bruneton,J.*PHARMACOGNOSIE,PHYTOCHIMIE,PLANTESMÉDICINALES(4EED.)*;LAVOISIER:Paris,France,2009;ISBN 2743019042.
76. Bekro,Y.-A.;MamyrbekovaBékro,J.A.;Boua,B.B.;Fézan,H.T.B.;Ehile,E.E.ÉtudeEthnobotaniqueetScreeningPhytochimique de Caesalpinia Benthamiana (Baill.) Herend. et Zarucchi (Caesalpinaceae). *Sci. Nat.* **2007**, 4, 217–225,Abidjan.
77. N'Guessan,K.;Kadja,B.;Zirih,G.;Traoré,D.;Aké-Assi,L.Screeningphytochimiquedequelquesplant esmédicinales ivoiriennesutiliséesenpaysKrobou(Agboville,Côte-d'Ivoire).*Sci.Nat.***2009**,6,1–15.<https://doi.org/10.4314/scinat.v6i1.48575>.
78. Akrou,A.;Chemli,R.;Chref,I.;Hammami,M.Analysisof theEssentialOilof ArtemisiaCampestris,L.*FlavourFragr.J.***2001**, 16, 337–339. <https://doi.org/10.1002/ffj.1006>.
79. Adams, R.P. *Identificationof Essential Oil Components by Gas Chromatography/Mass Spectrometry*; Allured publishing corporation Carol Stream, IL, USA, 2007; Vol. 456.
80. Babushok,V.I.;Linstrom,P.J.;Zenkevich,I.G.RetentionIndicesforFrequentlyReportedCompounds ofPlantEssentialOils.*J. Phys. Chem. Ref. Data* **2011**, 40, 043101. <https://doi.org/10.1063/1.3653552>.
81. Kovats,E.S.GasChromatographicCharacterization ofOrganicSubstancesintheRetentionIndexSystem. *Adv. Chromatogr.* **1965**, 1,229–247.
82. Singleton,V.L.;Rossi,J.A.ColorimetryofTotalPhenolicswithPhosphomolybdic-PhosphotungsticAcidReagents.*Am.J.Enol. Vitic.* **1965**, 16, 144–158. <https://doi.org/10.5344/AJEV.1965.16.3.144>.
83. Djeridane,A.;Yousfi,M.;Nadjemi,B.;Boutassouna,D.;Stocker,P.;Vidal,N.AntioxidantActivityofSomeAlgerianMedicinal PlantsExtractsContainingPhenolicCompounds.*FoodChem.* **2006**,97,654–660.<https://doi.org/10.1016/j.foodchem.2005.04.028>.
84. Price,M.L.;Scoyoc,S.V.;Butler,L.G.ACriticalEvaluationoftheVanillinReactionasanAssayforTanin inSorghumGrain.*J. Agric. Food Chem.* **1978**, 26, 1214–1218. https://doi.org/10.1021/JF60219A031/ASSET/JF60219A031.FP.PNG_V03.
85. Liu, M.H.; Otsuka, N.; Noyori, K.; Shiota, S.; Ogawa, W.; Kuroda, T.; Hatano, T.; Tsuchiya, T. Synergistic Effect of Kaempferol Glycosides Purified from Laurus Nobilis and Fluoroquinolones on Methicillin-Resistant Staphylococcus Aureus. *Biol. Pharm. Bull.* **2009**, 32, 489–492. <https://doi.org/10.1248/bpb.32.489>.
86. Oyaizu, M. Studies on Products of Browning Reaction. Antioxidative Activities of Products of Browning Reaction Prepared from Glucosamine. *Jpn. J. Nutr. Diet.* **1986**, 44, 307–315. <https://doi.org/10.5264/EIYOGAKUZASHI.44.307>.
87. Khiya,Z.;Oualcadi,Y.;Gamar,A.;Berrekhis,F.;Zair,T.;Hilali,F.E.L.CorrelationofTotalPolyphenolicContentwithAntioxidant Activity of Hydromethanolic Extract and Their Fractions of the Salvia Officinalis Leaves from Different Regions of Morocco. *J. Chem.* **2021**, 2021, 1–11. <https://doi.org/10.1155/2021/8585313>.
88. Driouche,A.;Baammi,S.;Zibouh,K.;Alkamaly,O.;Alnakhli,A.M.;Remok,F.;Saidi,S.;Amaia,R.;ElMakhoukhi,F.;Elomri,A.AStudyoftheSynergisticEffectsofEssentialOils fromOriganumCompactumandOriganumElongatumwithCommercial AntibioticsagainstHighlyPrioritizedMultidrug-ResistantBacteriafortheWorldHealthOrganization.*Metabolites***2024**,14,210.
89. Alam,A.;Jawaid,T.;Alam,P.InVitroAntioxidantandAnti-InflammatoryActivitiesofGreenCardamomEssentialOilandin Silico Molecular Docking of Its Major Bioactives. *J. Taibah Univ. Sci.* **2021**, 15, 757–768. <https://doi.org/10.1080/16583655.2021.2002550>.
90. Banerjee,P.;Eckert,A.O.;Schrey,A.K.;Preissner,R.ProTox-II:AWebserverforthePredictionofToxicityofChemicals.*Nucleic Acids Res.* **2018**, 46, W257–W263. <https://doi.org/10.1093/nar/gky318>.
91. Van Der Spoel, D.; Lindahl, E.; Hess, B.; Groenhof, G.; Mark, A.E.; Berendsen, H.J.C. GROMACS: Fast, Flexible, and Free. *J Comput Chem* **2005**, 26, 1701–